University of South Bohemia

Faculty of Science

Investigation of the gene *Dynactin subunit 2 (Dctn2)* in regulating the frequency of asymmetric cell divisions during mouse preimplantation embryonic development

MASTER´S THESIS

Bc. Michaela Kubíčková
2018

Supervisor of the master´s thesis: doc. Alexander W. Bruce, Ph.D.
Co-supervisor of the master´s thesis: Lenka Gahurová, Ph.D.

České Budějovice 2018

Kubíčková, M., 2018: Investigation of the gene *Dynactin 2 (Dctn2)* in regulating the frequency of asymmetric cell divisions during mouse preimplantation embryonic development, required to generate inner cells and drive successful cell lineage segregation and successful development. Mgr. Thesis, in English. – 64 p. Faculty of Science, University of South Bohemia, České Budějovice, Czech Republic.

Annotation

The aim of this study was to investigate the role of *Dctn2* in mouse preimplantation embryonic development, specifically its effect on the first cell fate decision, when the number of cells increases from eight to sixteen.

Prohlašuji, že svou diplomovou práci jsem vypracovala samostatně pouze s použitím pramenů a literatury uvedených v seznamu citované literatury.

Prohlašuji, že v souladu s § 47b zákona č. 111/1998 Sb. v platném znění souhlasím se zveřejněním své diplomové práce, a to v nezkrácené podobě elektronickou cestou ve veřejně přístupné části databáze STAG provozované Jihočeskou univerzitou v Českých Budějovicích na jejích internetových stránkách, a to se zachováním mého autorského práva k odevzdanému textu této kvalifikační práce. Souhlasím dále s tím, aby toutéž elektronickou cestou byly v souladu s uvedeným ustanovením zákona č. 111/1998 Sb. zveřejněny posudky školitele a oponentů práce i záznam o průběhu a výsledku obhajoby kvalifikační práce. Rovněž souhlasím s porovnáním textu mé kvalifikační práce s databází kvalifikačních prací Theses.cz provozovanou Národním registrem vysokoškolských kvalifikačních prací a systémem na odhalování plagiátů.

V Českých Budějovicích 12.dubna 2018

Acknowledgements

I owe my deepest gratitude to my supervisor doc. Alexander W. Bruce, Ph.D. His guidance in the research focusing on preimplantation mouse embryonic development has been essential during this work. I also express my warmest gratitude to my co-supervisor Lenka Gahurová Ph.D. who introduced me to the project. Without her continuous optimism concerning this work, encouragement and dedication to teach me the demanding laboratory methods this thesis would hardly have been completed.

My special thanks are extended to Mgr. Ondřej Gahura, Ph.D. for teaching me the western blotting methods. Materials provided by the Laboratory of Functional Biology of Protist, headed by RNDr. Alena Zíková, Ph.D., for western blotting were greatly appreciated. I also wish to acknowledge RNDr. Jindřich Chmelař, Ph.D. and his laboratory team for providing me with the PMJ2-R macrophages.

The research was performed at the University of South Bohemia, Faculty of Science, in České Budějovice and was mostly funded by the host lab´s GAČR grant, with a small contribution provided by the SGA grant 2017/18 awarded to Bc. M. Kubíčková.

Abstract

Preimplantation mouse embryonic development is defined as a developmental time-window started by oocyte fertilisation and concluding with uterine implantation, comprising a series of cleavage divisions that produce an increasing number of progressively smaller cells called blastomeres. Within this developmental time period three cell lineages are segregated. These are the trophectoderm, giving rise to the placenta, primitive endoderm later forming the yolk sac and epiblast building the embryo itself. Factors playing crucial roles during this process include the establishment of intra-cellular polarity and relative spatial cellular position that each contributes to the differential expression of key cell-fate influencing transcription factors. The segregation of the already mentioned cell lineages is accomplished in two successive waves of cell/blastomere internalisation occurring at the 8- to 16-cell and 16- to 32-cell transitions. During the 8- to 16-cell division, individual cells either divide to produce one polarised daughter cell on the outside and a second apolar cell encapsulated inside the embryo (an asymmetric division), or in an orientation that yields two outer polarised daughters (a symmetric division). The orientation of 8-cell stage divisions is known to be affected by the mitotic spindle angle and nuclear positioning, relative to, and along, the apical-basolateral axis but the exact mechanism regulating these processes remain largely unknown. mTOR signalling is known to regulate the translation of a subset of mRNAs containing a so-called TOP motif (5'UTR) and is also known to influence chromosomal segregation and meiotic spindle positioning in oocytes. Chemical inhibition of the mTOR pathway negatively influences inner-cell formation in 16-cell stage embryos, potentially via the translational regulation of mRNAs related to spindle orientation/ nuclear position. Interestingly, based on a published lists of TOP-containing RNAs, candidate genes have been identified and include the dynactin subunit 2 mRNA which is known to affect both spindle orientation and nuclear positioning. Experiments investigating the clonal knock-down of this candidate gene during the 8- to 16-cell stage transition are shown here to affect the generation of inner cells leading to reduced number of inner cells. This result implies to a requirement of *Dctn2* in the mechanism enabling the appropriate division of blastomeres and generation of inner cells required to support further embryo development.

Key words:

preimplantation mouse embryonic development, trophectoderm, primitive endoderm, epiblast, spindle orientation, nuclear positioning, candidate genes, dynactin subunit 2, mTOR signalling pathway.

Table of contents

Abbreviations

Apico-basal axis	A-B axis
Assisted Reproductive Techniques	ARTs
Bicaudal D2	BICD2
Bovine Serum Albumin	BSA
double stranded RNA	dsRNA
Dynactin-dynein	D-D
Dynactin subunit 2	Dctn2
eIF4E-binding protein 1	4E-BP1
Embryonic Stem cells	ESCs
Epiblast	EPI
Eukaryotic Elongation Factor 2 Kinase	eEF2K
Eukaryotic Initiation Factor 4E	eIF4E
FK506-binding protein	FKBP12
human Chorionic Gonadotropin	hCG
Immuno-fluorescent	IF
Integrin-Linked Kinase	ILK
In Vitro Fertilisation	IVF
In Vitro Transcription	IVT
Inner Cell Mass	ICM
Mammalian Target of Rapamycin	mTOR
Microtubule organizing centres	MTOCs
Paraformaldehyde	PFA
Peroxisome Proliferator-activated Receptor-γ	PPARγ
Phosphate Buffered Saline Tween	PBST
Pregnant Mare Serum Gonadotropin	PMSG

Primitive endoderm	PrE
p70 ribosomal S6 kinase 1	S6K1
Rhodamine dextran conjugated beads	RBDs
RNA interference	RNAi
Small Apical Domain	SAD
Sodium dodecyl sulfate	SDS
Sterol Regulatory Element Binding Protein 1	SREBP1
Terminal Oligopyrimidine Tract	TOP
Transcription factors	TFs
Trophectoderm	TE
Untranslated Regions	UTRs
Zygotic Genome Activation	ZGA

1 Introduction

1.1 Mouse preimplantation embryonic development

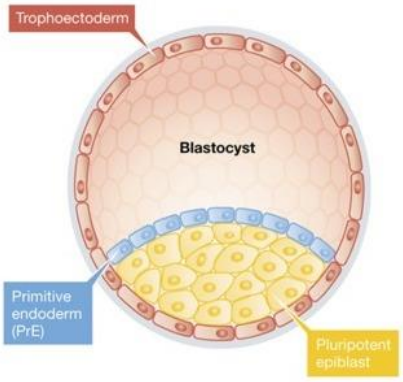

Fig. 1: A schema of the blastocyst stage mouse embryo containing the three cell lineages: TE in red, PrE in blue and EPI in yellow, and fluid filled cavity **(Mansour and Hanna, 2013).**

Mouse preimplantation embryonic development starts with oocyte fertilisation leading to the formation of a zygote and after 4.5 days concludes with uterine implantation of the embryo. The zygote undergoes a series of asynchronous cleavage division producing an increasing number of progressively smaller cells called blastomeres without changing the overall size of the embryo. After seven rounds of cell division a structure called the blastocyst (defined by a spherical epithelial tissue layer supporting a fluid filled cavity and a mass of inner cells) is created and the embryo is prepared for uterine implantation (Fig.1). This crucial window of early mouse embryonic development is analogous to the period during which derived human embryos are *in vitro* cultured prior to their transplantation to the uterus under certain assisted reproductive techniques (ARTs), such as *in vitro* fertilisation (IVF). Indeed, the preimplantation embryonic developmental period is devoted to the differentiation/ formation of extra-embryonic tissues, which are fundamental for implantation and post-implantation support of the embryo, as well as imparting specific cell differentiation and patterning signals to the developing embryo proper. As such, during this time, three distinct cell lineages are derived: the differentiating trophectoderm (TE) that will form the foetal part of the placenta, the primitive endoderm (PrE), that subsequently gives rise to parietal and visceral endoderm and later contributes to the yolk sac, and the pluripotent epiblast (EPI), comprised of progenitor cells required to build the embryonic foetus (Fig1). The three cell lineages arise as a result of two cell fate decisions, the first one in which outer-residing TE cells become segregated from the encapsulated cell population, ultimately forming the blastocyst inner cell mass (ICM), and the second decision in which EPI and PrE are specified and segregated from each other within maturing blastocyst ICM (Paria and Dey, 1990). The appropriate derivation of TE, PrE and EPI is crucial for the survival and normal development of the embryo, as exemplified by the need to form a fully

functioning TE, that is essential for embryo hatching and the complex molecular interactions between the uterus and the embryo during implantation (Cockburn and Rossant, 2010). However, the underpinning molecular mechanism of the derivation of these three cell lineages remain largely unknown and ill-characterised.

The whole process of early mouse embryonic development is driven by an, as yet, unidentified endogenous clock that ensures that certain morphological events (*e.g.* embryo compaction and cavitation or intra-cellular apical-basolateral polarisation) coincide with particular developmental cell cycles (Johnson, 2009). This is exemplified by experiments in which separated blastomeres of the 2-cell stage embryos still independently follow the same clock of development transitions as intact embryos (Morris, Guo and Zernicka-Goetz, 2012). It is noteworthy that the first two cell cycles of preimplantation mouse embryo development last significantly longer than those that come subsequently, being specific, 20 hours versus 12 hours in length (Artus and Cohen-Tannoudji, 2008).

Following oocyte fertilisation, the mouse zygote initially relies on maternal stores of mRNAs and proteins but by the end of the 1-cell stage its own genome becomes transcriptionally activated by a minor burst of transcription followed by the major burst at the end of the 2-cell stage (Fig.4b). This developmental breakthrough is known as zygotic genome activation (ZGA) and is precocious in mice versus other mammalian model species. Simultaneously, the maternal mRNAs are actively degraded during the 2-cell stage, in contrary to maternally provided proteins that can sometimes be maintained long into the preimplantation stage development period (Zernicka-Goetz, Morris and Bruce, 2009).

In the time window between the cleavage of the zygote and the 8-cell stage, embryos are highly adaptable to changes, such as removal, addition or rearrangement of blastomeres. For instance, if one of the blastomeres is removed or destroyed, the remaining cell can compensate for its loss and support full and proper development (Tarkowski, 1959; Morris, Guo and Zernicka-Goetz, 2012). Whereas, individual cells separated from the 4- or 8-cell stage are not alone able to develop beyond the uterine implantation stage (Tarkowski and Wróblewska, 1967; Rossant, 1976). However, such cells are still able to contribute to all blastocyst cell lineages and foetal tissues when combined with other cells, equivalently developmentally staged, in embryo chimeras; demonstrating that they still retain their full developmental potential (Kelly, 1977; Piotrowska-Nitsche and Zernicka-Goetz, 2005). However, this fact does not necessarily indicate that the embryo has not yet started the process of individual blastomere differentiation by these early cleavage stages, but rather

shows the cells have not yet become irreversibly restricted in fate (*i.e.* they remain developmentally plastic). This is supported by pioneering experiments with chimeras, whereby the aggregation of two equivalently developmentally staged preimplantation embryos is able to regulate the developmental programme and thus generate of a single viable individual (Tarkowski, 1961). This remarkable plasticity, that counts as one of the main features of mammalian development, is referred to as 'regulative development' and is lost after the complete specification and segregation of the three cell lineages by the late blastocyst stage.

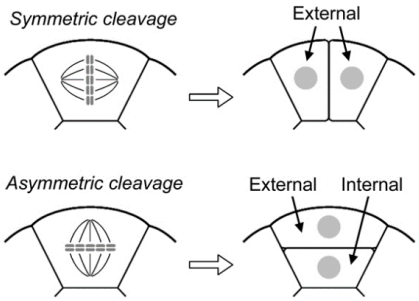

Fig. 2:A schema for the symmetric and asymmetric cleavage division orientations in mouse preimplantation stage embryos (Marikawa and Alarcón, 2009): Symmetric division pattern, typified by a cleavage axis that is oriented in parallel to A-B axis, resulting into two external and polarised blastomeres and asymmetric cleavage orientations, defined by the cleavage plan being perpendicular to the A-B axis, to result in one apolar internal and one polarised external blastomere.

Although the establishment of inter-blastomere variability is recognised as a prerequisite of functional blastocyst formation and cell lineage specification, up until the 8-cell stage all blastomeres of early cleavage mouse embryo appear morphologically identical, exhibiting a loosely associated inter-cell connectivity. However, there is some debate as to whether there exists some level of initial and functionally important molecular heterogeneity between the blastomeres, as some experimental evidence suggests certain blastomeres maybe developmentally biased to preferentially contribute towards one or another blastocyst cell lineage (Zernicka-Goetz, 2004). Moreover, other modelling experiments based on the clonal inhibition of TE cell fate initiation within the cleavage stage embryo have shown that the ICM residing progeny arising from such TE-inhibited clones, preferentially contribute to the EPI, due to reduced expression of required PrE marker genes, such as *Dab2*, *Lrp2* and *Fgf2* (Mihajlović, Thamodaran and Bruce, 2015). Hence, supporting the hypothesis that early inter-blastomere heterogeneities can have functional significance for later blastocyst cell lineage segregation.

Before the onset of the first cell fate decision all blastomeres are developmentally plastic and highly influenced by cell-cell interactions. At the 8-cell stage, blastomeres undergo the process of intra-cellular polarisation, resulting from the asymmetric distribution of specific intra-cellular components and the establishment of an apico-basal

axis (A-B axis) of polarity in each blastomere. This process of polarisation is concomitant with a process called compaction, the first morphogenetic event in preimplantation embryonic development, whereby intracellular contact is increased and as a result individual blastomeres become more flattened and results in the formation of two distinct membrane domains differentially enriched by the presence of specific polarity protein factors: *i.e.* the cell contactless apical domain and the basolateral domain that shares cell-cell contacts. Blastomere compaction and polarisation by the late 8-cell stage is essential for the subsequent formation of two spatially and molecularly (in terms of the extent of apical-basolateral polarity) different populations of cells. These cells will either allocate to the encapsulated inside compartment or remain on the outside surface of the embryo, consequent to two successive waves of cell division that could potentially result in daughter cell internalisation (*i.e.* the first wave occurring at the 8- to 16-cell stage transition and the second, relating to only outer cells, when the number of blastomeres increases from 16 to 32). Alternatively expressed, after compaction and polarisation the embryo undergoes cell cleavage divisions that will, depending on the orientation of the mitotic spindle, result in the generation of either outer or inner cells (Dard, Louvet-Vallée and Maro, 2009). As such, 'asymmetric' divisions are correlated with spindle poles aligning with the A-B axis (of the 8-cell or outer 16-cell stage blastomere) and result in the generation of one apical-basolaterally polarised outer daughter cell and one apolar inner cell. Alternatively, the blastomeres can also divide

symmetrically, whereby the mitotic spindle orientation is perpendicular to the A-B axis, and the cleavage plane is oriented in parallel to it. Such cleavage orientations yield two polarised outer daughter cells, each containing a contactless polarised apical domain (Fig.2) (Dard *et al.*, 2008; Zernicka-Goetz, Morris and Bruce, 2009). It has been reported that the symmetric divisions which are perpendicular to the A-B axis can occur in cells that exhibit both basal and apically positioned nuclei, whereas asymmetric divisions typically only occur in cells in which the nuclei is positioned relatively basally (Ajduk, Biswas Shivhare and Zernicka-Goetz, 2014)**.** However, it is also important to note that some blastomeres that were initially segregated to outer positions can later become encapsulated by active cell movements, related to inter-blastomere heterogeneities in cortical tension that themselves are related to the extent of inherited apical-basolateral polarity resulting from relatively oblique angles of cell division (Anani et al. 2014; Maître et al. 2016; Korotkevich et al. 2017; Mihajlović and Bruce 2017).

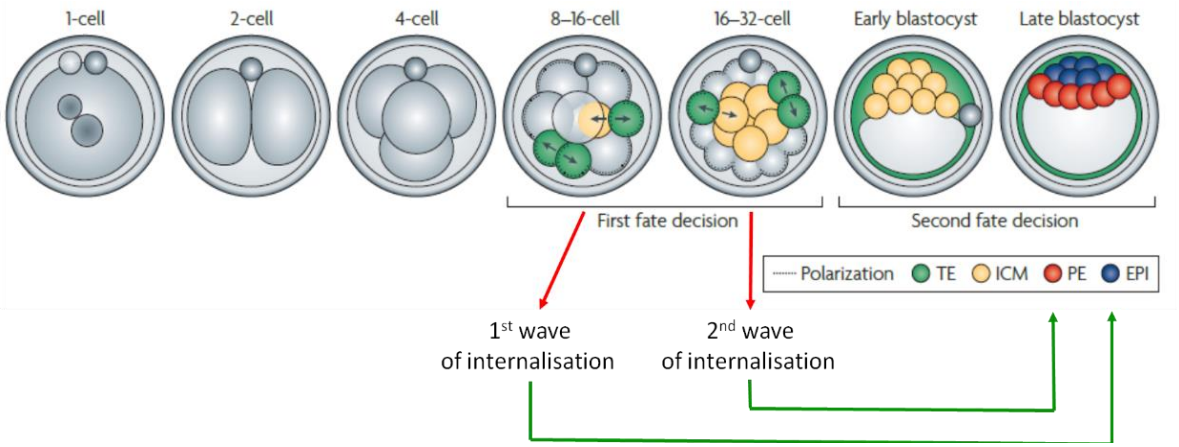

Fig. 3: **The two waves of cell internalisation emerging during mouse preimplantation embryonic development (adapted from Zernicka-Goetz et.al., 2009):** The first wave of internalisation occurs from the 8-cell stage, when all blastomeres are morphologically equal and the first outer and inner cells arise, resulting into 16 cells. The second wave of internalisation take place from the 16-cell stage (experimental evidence suggests primary ICM founder cells can be biased to preferentially contribute to the EPI whereas secondary ICM founders preferentially contribute to the PrE – see arrows).

It is proposed that ICM founder cells internalized consequent to the first wave of internalisation (*i.e.* the 8-cell to 16-cell stage transition), and hence minimally exposed to TE promoting differentiation cues, are biased to ultimately form the EPI, whilst those internalised later, following the 16-cell to 32-cell transition, are more likely to form the differentiating PrE (Morris *et al.*, 2010; Mihajlović, Thamodaran and Bruce, 2015). Cells contributing to PrE become morphologically defined in the late blastocyst stage as a layer of epithelial cells at the surface of the ICM, facing the fluid filled cavity, whereas EPI specified cells remain in the deeper layers of the ICM; cell fate commitment to either PrE or EPI is established by the time of implantation at the late blastocyst stage by E4.5 (Zernicka-Goetz, Morris and Bruce, 2009).

The arising, from the 8-cell stage, inter-blastomere differences in the position (inner/outer) and intra-cellular organisation (polarised/non-polarised) are responsible for the gradual specification and segregation of the first two cell lineages: TE and ICM (Fig.4a). However, such spatial segregation and differential polarisation status does not necessarily mean irreversible specification towards TE or ICM fates. This is highlighted in experiments where both inner and outer cells removed from their original relative spatial positions in 16-cell stage were placed in the opposite spatial environment in chimeras and were shown to still be capable of reprogramming their fate according to their new position; thus, demonstrating developmental plasticity and confirming initial relative spatial separation and divergent polarisation status is not accompanied by irreversible cell fate

commitment at that stage. This fact indicates that all blastomeres in the 16-cell stage remain, to a certain extent, pluripotent. In fact, after the re-aggregation of a uniform population of either outer or inner cells into 16-cell clusters, blastomeres are able to develop into morphologically normal blastocysts that result in fertile offspring after uterine transfer. However, this plastic ability is lost by the late 32-cell stage, when the blastomeres strictly belong to committed TE or ICM and thus can-not switch their fate (Suwińska *et al.*, 2008).

At the 32-cell (E3.5) stage, after the formation of an outer epithelium of committed TE cells, a fluid-filled cavity (sometime called the blastocoel) that is the morphologically defining feature of the blastocyst, is formed. This process is ensured by the creation of an osmotic gradient created by Na^+ ion influx, mediated by apically localised Na^+/H^+ exchangers in the TE, and Na^+/K^+ ion efflux via ATPases positioned on the basolateral TE membrane (Eckert *et al.*, 2004). The integrity of the growing cavity is maintained due to the concomitant maturation of tight junction assembly between neighbouring TE cells, which had been initiated earlier in development, during compaction. Note that progressive expansion of the cavity volume is required for the blastocyst to ultimately emerge/ hatch from its proteinaceous protective shell, the *zona pellucida*, and complete uterine implantation; hence failures in TE specification are invariably lethal to the embryo. Furthermore, cavity formation is asymmetrically positioned in relation to the inner cells of the embryo, thus positioning the nascent ICM at one pole and defining the embryonic and abembryonic axis of the embryo; the pole containing the ICM is defined as the embryonic pole whereas the pole defined by the cavity is referred to as being abembryonic. As such, this positioning also defines the mural TE as being that which is in contact with the fluid-filled cavity at the abembryonic region and the polar TE overlaying the ICM at the embryonic pole.

TE specification and blastocyst cavity formation are followed by the specification and segregation of ICM cells into the PrE and EPI lineages. The PrE forms as a single cell monolayer at the superficial surface of the ICM that is in contact with the cavity, whereas the EPI is comprised of a mass of cells centrally positioned in the ICM, between the epithelialized layers of the PrE and polar TE. The precursors of these two cell lineages within the ICM emerge from initially uncommitted cells at the early blastocyst stage that then resolve into a so-called ´salt-and-pepper´ pattern, defined by the mutually exclusive inter-cellular expression pattern of early PrE markers and pluripotency related transcription factors. These fate specified progenitors gradually segregate into the recognisable PrE and

EPI tissue layers of the late blastocyst via a combination of active cell movement and selective apoptosis (plus some inductive changes in cell fate related gene expression) (Dard, Louvet-Vallée and Maro, 2009; Zernicka-Goetz, Morris and Bruce, 2009; Bruce and Zernicka-Goetz, 2010; Cockburn and Rossant, 2010; Schrode *et al.*, 2013). The mechanism governing the specification and derivation of the PrE and EPI is known to be related to FGF signalling (Chazaud *et al.*, 2006; Nichols *et al.*, 2009; Yamanaka *et al.*, 2010; Frankenberg *et al.*, 2011; Kang *et al.*, 2013; Kang, Nachtrab and Poss, 2013; Morris *et al.*, 2013; Thamodaran and Bruce, 2016; Bessonnard *et al.*, 2017) and moreover it has been shown that differences in the level of *Fgf4* and *Fgfr2 gene* expression levels have been detected in blastomeres generated within either the first or second wave of cell internalisation, supporting the theory that specification of ICM founder cells to either PrE or EPI fates is partly influenced by the timing of the inner cells generation (although it was also reported that the total number of cells generated during each wave of internalisation is also important (Krupa *et al.*, 2014)).

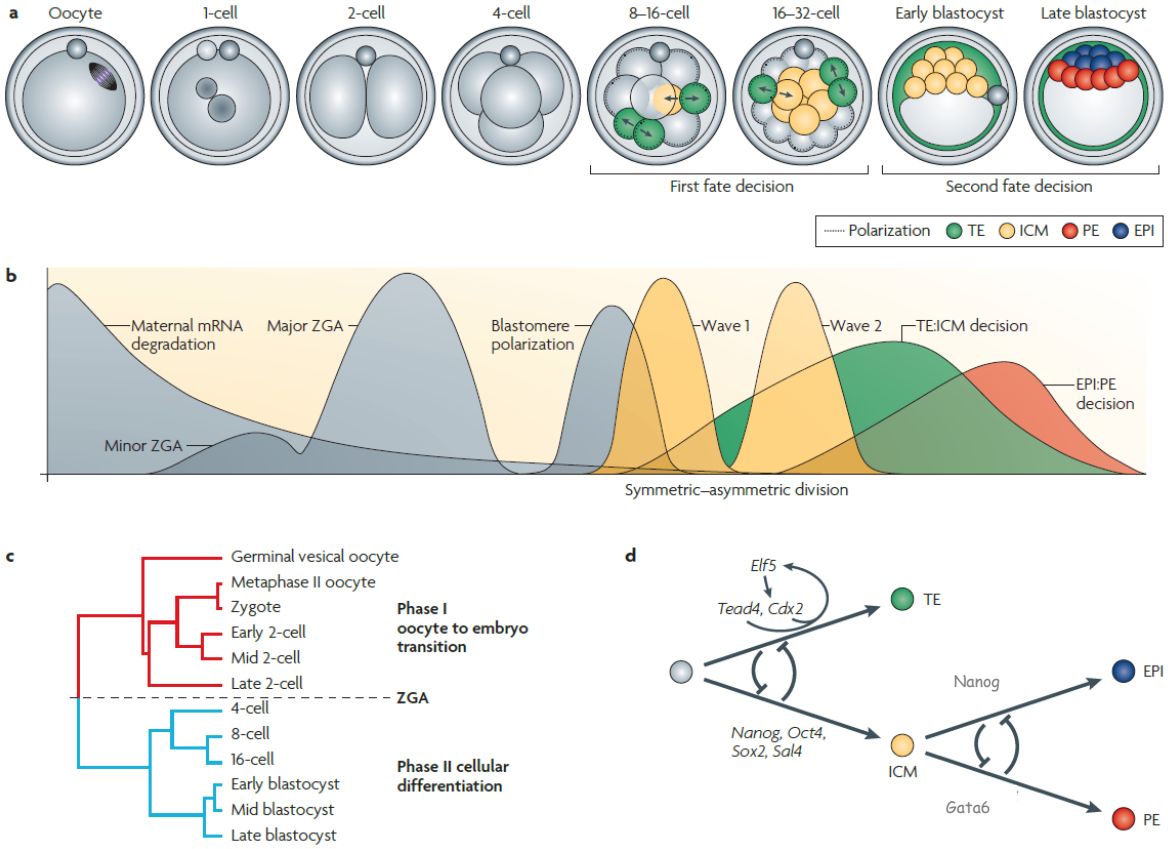

Fig. 4: Mouse preimplantation embryonic development (adapted from Zernicka-Goetz et.al, 2009): a. The increasing number of blastomeres throughout the individual stages of the embryo in the course of the preimplantation development. TE is set apart from ICM in the first cell fate decision and PrE and EPI are segregated during the second cell fate decision. **b.** The dynamic of the ZGA starting with the maternal-to-zygotic transition and proceeding with the dominant persistence of the zygotic genome. **c.** The expression level of mRNAs during preimplantation development orderly structured into clusters. **d.** The known and key transcription factors (TFs) of preimplantation developmental, during the specification and segregation of the TE (Tead4, Cdx2 and Elf5) and ICM (Nanog, Oct4, Sox2 and Sal4) and then during the specification and segregation of PrE (Gata6) and EPI (Nanog).

The preimplantation developmental period in mice is driven by a gradient of transcription factors (TFs), which fall into two groups: TFs retaining pluripotency such as Oct4 (Schöler *et al.*, 1990), Sox2 (Avilion *et al.*, 2003) and Nanog (Chambers et al. 2003) and TFs providing differentiation such as Cdx2 (Niwa *et al.*, 2005; Strumpf, 2005; Jedrusik *et al.*, 2008), Eomes (Russ *et al.*, 2000) and Tead4 (Yagi *et al.*, 2007; Nishioka *et al.*, 2008). The cell fate decisions are, apart from other factors, affected by the relative expression level of the abovementioned TF proteins. Specifically, during the first cell fate decision, cells that will ultimately contribute to the TE are predominantly affected by transcriptional gene expression regulation that promotes differentiation, mediated by Tead4 and Cdx2 (Niwa *et al.*, 2005; Strumpf, 2005). Conversely, in the ICM, TF genes such as *Sox2* and *Nanog* are up-regulated and thus promote pluripotency and differentiation is suppressed (Mitsui *et al.*, 2003). During the second cell fate decision where PE and EPI are

specified and segregated from early blastocyst ICM cells that remain uncommitted, key TFs also play an important role; specifically Nanog and Sox2 by preserving/ ensuring pluripotency in EPI and Gata6 by driving the expression of genes required to specify and segregate the PrE, including the sequential activation of other required TF genes including *Sox17*, *Gata4* and *Sox7* (Fig.4d) (Zernicka-Goetz, Morris and Bruce, 2009).

1.2 The first cell fate decision and cell internalisation bias

Within the first cell fate decision, TE and ICM lineages segregate from each other. These two cell lineages become conclusively committed to their appropriate lineages during the 32-cell stage (at E3.5) (Suwińska *et al.*, 2008), which is proposed to be the time point by which the first cell fate decision is fully committed and made. The specific mechanistic details explaining how this is achieved remain predominantly unknown. However, two historical models attempting to explain the first cell fate decision have been proposed. The first is the "positional" model (sometimes referred to as the "inside-outside" model) which proposes that cell-specific environmental cues (differential between inner and outer positioned cells) underpin the separation of fates. This view was supported by experiments in which disaggregated blastomeres that had been originally allocated to one spatial position were found to appropriately select the correct cell fate when placed in the opposing spatial environment; hence, inside cells develop into ICM, while outside cells develop into TE (Tarkowski and Wróblewska, 1967). The second model is the "polarity" model and suggests that a cell´s inheritance of the apical-basolateral polarity (typified by the presence of a contactless polarised apical domain), or not, determines subsequent cell fate; so that polarised cells (residing on the outside of the embryo) differentiate to TE and apolar (inner) cells eventually form the ICM (Johnson and Ziomek, 1983; Beck *et al.*, 2003).

The relative spatial segregation of blastomeres within the developing mouse preimplantation stage embryo (occurring in two successive cleavage transitions; *i.e.* internalisation following the 8- to 16-cell transition and outer cell internalisation resulting from the 16 to 32-cell transition) is fundamental to successful execution of the first cell fate decision and has been shown to be dependent on the type/ orientation of the cleavage divisions themselves (i.e. symmetric or asymmetric), which is largely affected by the mitotic spindle orientation (Bergstralh, Dawney and St Johnston, 2017). However, other factors have been shown to influence spindle orientation and include the extent and orientation of the cells A-B axis of polarity (Korotkevich *et al.*, 2017) and the position of

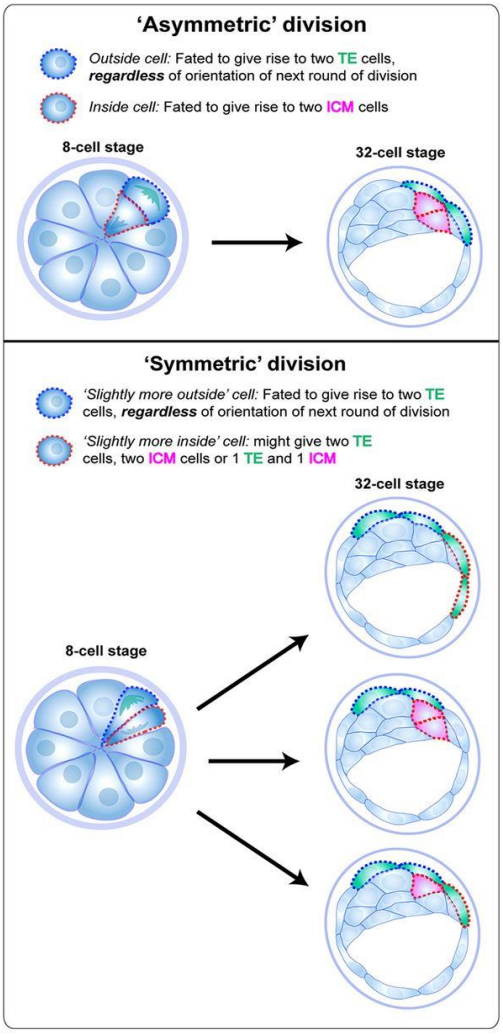

Fig. 5: Depiction of the connection between the angles of division and TE versus ICM fate (Watanabe *et al.*, 2014).

nuclei along the A-B axis immediately prior to division (Ajduk, Biswas Shivhare and Zernicka-Goetz, 2014); whereas other factors, such a cells intrinsic capacity to internalise (negatively correlated with a cell's extent of apical–basolateral polarity) (Samarage *et al.*, 2015) can also affect the relative spatial segregation of cells.

As already stated, there are in general two basic types of mitotic spindle orientation in 8-cell and outer cells of 16-cell stage mouse embryos, that are determined by their relative alignment to the radial A-B axis in each individual cell; *i.e.* symmetric or asymmetric (leading to the delineation of outer TE and inner ICM founders - Fig.5). As such, individual cells can divide to produce one polarised daughter cell on the outside and a second apolar cell encapsulated within the embryo; in this case the mitotic spindle is oriented in parallel to the apico-basal axis (A-B axis), thus the resulting cleavage plane is perpendicular to the A-B axis. Such a cleavage is referred to as an asymmetric division and results in the generation of one outer and polarised cell contributing to the differentiating TE and one apolar inner cell supporting the pluripotent ICM. In contrast, cells can also divide symmetrically so that the cleavage plan is parallel, and the mitotic spindle orientation perpendicular, to the A-B axis. Such division yields two outer polarised cells contributing to the differentiating TE (Anani *et al.*, 2014). However, in cases where the mitotic spindle neither aligns with the A-B axis nor is strictly perpendicular to it, so-called oblique divisions occurs. Therefore, oblique types of division are characterised by a non-equal inheritance of the polarised apical and adhesive basolateral domains by each daughter cell (that each initially occupy outer spatial positions). However, if a produced daughter cell does not inherit a sufficiently large component of the apical domain it will most often be encapsulated later in the development and thus form an inner cell. Such outer cells, resulting from oblique divisions, are classified as "small apical domain" (SAD)

containing cells (Zernicka-Goetz, 2005). Intra-cellular apical-basolateral polarity is closely associated with the orientation of the mitotic spindle orientation during cell division and the key role of the polarised apical domain during the first cell fate decision was underlined by the experiments using transplantations of the polarised apical domains, to initially apolar recipient cells. Such experiments showed that the attainment of an explanted polarised apical domain is sufficient to drive a resulting asymmetric cell division, perpendicular to the newly acquired A-B axis, even in disaggregated single blastomeres. However, it is important to note that in the *in vivo* embryo context there is an interplay between the other decisive factors that are also undoubtedly important (Korotkevich *et al.*, 2017).

It has been reported that the nuclei in 8-cell stage mouse embryo blastomeres migrate, to varying degrees, from apical to more basal positions, in a microtubule- and kinesin-dependent manner, and moreover that the extent of this movement prior to nuclear envelope breakdown at cell division affects outer/inner cell spatial segregation. Specifically, that cells entering mitosis with relatively apically positioned nuclei invariably divide symmetrically, whilst asymmetric divisions only occur in blastomeres with a basally positioned nucleus; although it is still possible symmetric divisions can emerge from such cells (Ajduk, Biswas Shivhare and Zernicka-Goetz, 2014). Thus, factors that can potentially affect the degree/ ratio of apical-basal nuclear positioning are theoretically able to impinge on the spatial segregation of TE and ICM progenitor cells, in the developing preimplantation stage mouse embryo.

Another important factor regulating the internalisation of cleavage stage embryonic cells is their relative cortical tension. Experiments studying the mechanical forces within the early mouse embryo have shown apical constriction, generated via the contractility of the action-myosin cell cortex underlying the contactless apical domain, is also responsible for allocating inner cells during the first cell fate decision. The subcellular heterogeneities in tensile forces observed between, and dispersed between, neighbouring cells are also centrally involved in allocating individual cells to the inner cell embryo compartment (Samarage *et al.*, 2015). Furthermore, the crucial role of actomyosin contractility has also been independently demonstrated and developed via experiments using maternal myosin (Myh9)-knockout chimeric embryos, where the induced loss of contractility resulted in the expression of ICM-like markers irrespective of the relative position of the cell within the chimeric embryo. Therefore, it was concluded that actomyosin contractility in connection with cell polarity and the expression of cell fate related TFs contributes to the robust self-organisation of blastomeres in the developing embryo by the blastocyst stage (Maître *et al.*,

2016). Highly regulated and specific transcriptional circuits are inherently connected with the first cell fate decision because they are closely related to the extent of an individual cell's apical-basolateral polarity. This has been demonstrated for the mRNA transcript of the TE-related TF Cdx2, that asymmetrically accumulates at the polarised apical domain of 8-cell and outer-16-cell stage blastomeres and is thus potentially differentially distributed between daughter cells according to the type of the ensuing cell division (*i.e.* symmetric/asymmetric). In cases when the cell divides symmetrically, the Cdx2 mRNAs become equally distributed into both outer daughter cells, thus both daughter cells inherit the same potential to express a TE-appropriate gene expression program. Whereas if an asymmetric (or even oblique) division occurs, only one (outer-residing) daughter cell inherits all (or the majority) of the apically localised Cdx2 mRNA and thus initiates/ maintains TE differentiation. The other daughter cell (partitioned to the inner compartment) does not inherit any Cdx2 mRNA and therefore develops into an ICM progenitor (or in the case of oblique divisions inherits very little Cdx2 mRNA to effect cell fate choice when the cell is ultimately internalised) (Jedrusik *et al.*, 2008; Skamagki *et al.*, 2013). Indeed, consequent to symmetric cleavage divisions, both cell polarity and TE cell fate have been reported to mutually reinforce each other, as increased expression of Cdx2 has been shown to enhance cell polarity (Jedrusik *et al.*, 2008), which in turn is argued to augment the asymmetric distribution of apically localised Cdx2 mRNAs (Skamagki *et al.*, 2013) (Fig.6a). Whereas in inner cells, the expression of the pluripotency related TFs Nanog and Oct4 is reinforced by a lack of transcriptionally repressive Cdx2 mediated regulation (Niwa *et al.*, 2005; Zernicka-Goetz, Morris and Bruce, 2009). This represent a prescient example of the feed-back loop principle, that is essential for the functioning of TF driven cell-fate regulating circuitries within the first cell fate decision (Fig.6b).

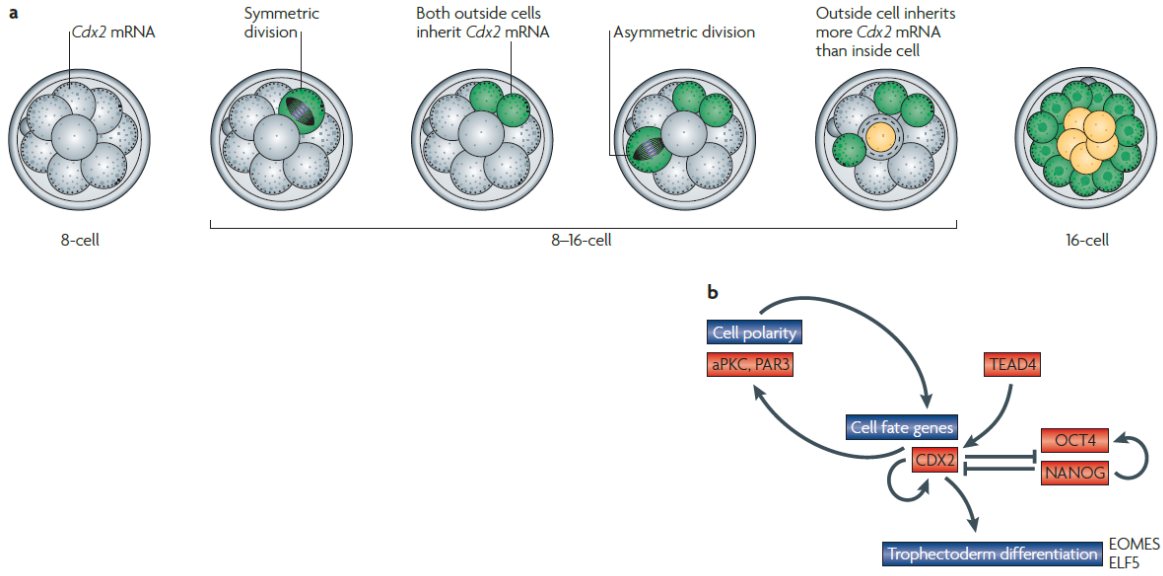

Fig. 6: **The depiction of the molecular basis within the first cell fate decision (Zernicka-Goetz et al. 2009): a.** The asymmetric distribution of Cdx2 mRNAs at the polarised apical domain that according to the orientation of subsequent cleavage divisions acts to bias newly generated daughter blastomeres to become either outer TE (driven by polarised Cdx2 localised transcripts) or inner ICM cell founders **b.** The feedback loop principle of the cell polarity, cell fate and TF expression (Cdx2, Nanog and Oct4) that cooperates to co-ordinately specify the segregated first cell fates of mouse preimplantation embryo development.

Taking into consideration of all the factors that have been reported to bias blastomeres towards occupying their relative spatial positions within the developing mouse embryo and consequently adopting an appropriate cell fate (in the context of the first cell fate decision) it appears this window of early development is extremely complex and based on the delicate interplay of several crucial morphological events (*e.g.* compaction and polarisation, spindle orientation, relative intra-cellular contractile and tensile forces *etc.*). Therefore any further functional insight that can aid the identification of key factors and genes involved in the specification and segregation of the first cell fates, can only serve to illuminate this period of development and further our understanding of its inherent complexities.

1.3 The mammalian target of rapamycin (mTOR) signalling pathway and its role in mouse embryonic development

The mTOR signalling pathway has been proven as a very important regulator of many essential processes occurring in the cell, such as growth, metabolism, proliferation and survival. This regulation is achieved through intra-cellular and extra-cellular signals acting

through a defined set of signal molecules that are organized into two multi-protein complexes called mTORC1 and mTORC2 (Guertin and Sabatini, 2007).

The mTORC1 complex is considered as a master regulator of cellular metabolism and is intimately connected to the regulation of cell growth. It is essential for many anabolic processes, including biosynthesis of proteins, lipids and organelles and the complementary restriction of catabolic processes, such as autophagy. These findings come from observations of experiments employing the pharmacological mTOR inhibitor rapamycin, that binds to FK506-binding protein (FKBP12), thus inhibiting mTORC1 activity (Guertin and Sabatini, 2007); as such mTORC1 is classified as being a rapamycin-sensitive mTOR complex. However, mTORC2 is unable to interact with rapamycin and is thus classified as a rapamycin-insensitive complex. Although this classification might not be entirely correct in all contexts, as it has been shown that chronic rapamycin treatment can indirectly block the assembly of the mTORC2 complex and thus inhibit its activity in some cases (Sarbassov *et al.*, 2006).

With regard to the regulation of protein synthesis, mTORC1 promotes translation by the phosphorylation of eIF4E (eukaryotic translation initiating factor 4E; part of the ^{7}methyl-guanasine cap binding complex, eIF4F) inhibitory binding protein 4E-BP1 and the p70 ribosomal S6 kinase 1 (S6K1). The phosphorylation of 4E-BP1 prevents the binding of 4E-BP1 to eIF4E, thus promoting cap-dependent translation (Richter and Sonenberg, 2005). Furthermore, the phosphorylation of S6K1 causes its activation and in turn results in the reinforcement of mRNA biogenesis, cap-dependent translation and the translation of ribosomal proteins, for instance, ribosomal protein S6 and eukaryotic elongation factor 2 kinase (eEF2K); to promote protein synthesis/ translation (Ma and Blenis, 2009). mTORC1 is also essential for lipid synthesis and is required for cell growth (that by its inherent nature requires extra lipid membrane generation) and proliferation. This has been confirmed by experiments based on rapamycin mTOR inhibition that show mTORC1 activity is required to activate and enable sterol regulatory element binding protein 1 (SREBP1) and peroxisome proliferator-activated receptor-γ (PPARγ) TFs to direct the enhanced transcription of genes encoding proteins involved in lipid and cholesterol homeostasis (Kim and Chen, 2004).

It has been reported, that mTORC1 inhibition causes increased levels of autophagy (a destructive process within the cell securing sequestration and disassembly of intra-cellular dysfunctional components), whilst the experimental stimulation of mTORC1 is associated with reduced autophagy (Codogno and Meijer, 2005); thus highlighting how the mTOR

pathway (and mTORC1 in particular) can play an important cell survival role, when nutrients availability is limited and the degradation of protein complexes and organelles might be required to sustain essential anabolic processes. However, the increased levels of autophagy mediated protein degradation caused by rapamycin inhibition is certainly disadvantageous for the cell, if left unchecked for prolonged periods.

To date, there have been no studies investigating the potential roles of mTOR pathway during early mammalian embryonic development (before blastocyst formation) nor its potential to impact upon both of the two cell fate decisions described above. However, several groups have reported various roles for mTOR in later preimplantation/ peri-implantation development and post-implantation. For example, the inhibition of mTOR activity can induce a reversible diapause in the development of the mouse blastocyst, as well as in cultured embryonic stem cells (ESCs). Such paused blastocysts retain their pluripotency and are able, once relieved of mTOR inhibition, to develop into live and fertile adults. The induction of diapause, either in the *in vivo* or *ex vivo* contexts, causes significant reductions in mTOR activity, global transcription and translation, as well as impaired activity of genes associated with the deposition/ removal of epigenetic post-translational histone modifications. Importantly, this research indicates that mTOR activity is able to regulate the developmental timing window within the critical peri-implantation developmental context (Bulut-Karslioglu *et al.*, 2016).

Embryonic lethality associated with mTOR inhibition has been comprehensively demonstrated by induced genetic null experiments targeting the *mTOR* gene. The effect of the mutation was investigated in both the homozygous and heterozygous states. Mice carrying the heterozygous *mTOR* mutations were found to not display any overt phenotypes, compared to the wild-type control groups, however, their fibroblasts were shown to contain 50% less of the specific mTOR protein and reduced levels of S6K1 T389 phosphorylation (a direct target substrate of mTOR – see earlier). By contrast, mice with the homozygous mutation displayed a developmental arrest at E5.5 that was associated with smaller sized embryos, defective ICM proliferation and a limited level of trophoblast cells; thus contributing to the aberrant developmental arrest phenotype (Gangloff *et al.*, 2004).

Furthermore, the inhibition of mTOR by the chemical inhibitor rapamycin or by a gene loss-of-function mutation in the *mTOR* itself leads to phenotype discrepancies in the mouse embryos examined 9.5 days postcoitum; as was demonstrated by experiments investigating the serine/threonine kinase activity of mTOR (known to mediate the cellular response to

mitogens through phosphorylation dependent signalling to SK61 and 4E-BP1, that causing increased translation of cellular mRNAs to thus positively affect cell proliferation). In these experiments, rapamycin inhibition was performed by intra-peritoneal injections of pregnant female mice 5.5 days postcoitum. At E9.5 the rapamycin treatment was shown to cause G1 cell cycle arrest in mouse embryonic development. The same effect was repeated in mTOR mutated embryos, collectively providing evidence about the teratogenic potential of mTOR mutation/inhibition on tissues requiring rapid proliferation during embryonic development; such as telencephalon, ventral body walls and limb buds (Burnett *et al.*, 1998).

The crucial role of mTOR in regulating cell growth and proliferation in mouse embryo and embryonic stem cells has also been exemplified in experiments based on the genetic disruption of the kinase domain of mouse, the *mTOR* gene, by homologous recombination in the mouse embryo. Moreover, the phenotype was examined in mouse embryos at 8.5, 9.5, 10.5 and 12.5 days postcoitum and demonstrated that whilst heterozygous mutant mice were overtly normal and fertile, embryos harbouring the homozygous mutation died soon after implantation (5.0 days postcoitum), due to impaired cell proliferation in both embryonic and extraembryonic tissues; a result that phenocopied that described above (Gangloff et al. 2004). Furthermore, the deletion of six amino acids from the C-terminus of mTOR, that are required for the activation of the substrate S6K1 kinase in embryonic stem cells, also resulted in decreased cell size and reduced proliferation and eventual arrest in ESC models (Murakami *et al.*, 2004). Hence, demonstrating that mTOR is indispensable during the mouse embryonic development based on cell growth and proliferation securing the proper formation of the embryonic and extraembryonic tissue.

1.4 The role of mTOR in candidate gene translation

One of the interesting and multiple roles of mTORC1 signalling pathway is the regulatory role it plays in the translation of a subset of mRNAs that contain a so-called terminal oligo-pyrimidine tract (TOP) motif, in their 5′ untranslated regions (5'UTRs) (Laplante and Sabatini, 2009; Thoreen *et al.*, 2012). The main structural features of TOP-containing mRNAs are defined as: (i) C residues followed by a stretch of 4 to 14 pyrimidines, (ii) a comparable ratio of C and U residues within the pyrimidine stretch of most TOP-motif containing mRNA members, (iii) a CG rich sequence downstream of the 5′TOP motif itself and (iv) a significantly conserved 5′TOP motif (same or very similar sequence within the TOP motif in the individual genes among mammals) and neighbouring transcribed sequence (Meyuhas and Kahan, 2015). The exact mechanism of the translation

regulatory role played by TOP-motifs is not fully understood, but nevertheless has been addressed by Hamilton et al. in experiments assaying the polysome associated fraction of cellular mRNAs (*i.e*. transcripts actively associated with translating ribosomes) via cDNA microarray analysis. Specifically, the authors showed that required translation of ribosomal protein related mRNAs is dependent on cis-elements located within the 5´UTR region that are in proximity to TOP-motifs (Hamilton *et al.*, 2006). Additionally, the general translational regulation of gene mRNAs by mTOR is also known to be regulated via the binding/ assembly of the eukaryotic initiation factor 4E (eIF4E) into the greater/trimeric complex known as the mRNA 7-methyl-guanosine-cap binding complex (eIF4F), via the phosphorylation of the eIF4E-binding protein 1 (4E-BP1 – referred to above) (Fig.7) (Lin *et al.*, 1994; Pause *et al.*, 1994; Fadden, Haystead and Lawrence, 1997). Accordingly, 4E-BP1, which belongs to a family of three small proteins in mammals, functions as an inhibitor of translational initiation, due to its ability to bind and inactivate eIF4E (*i.e.* prevent its assembly into the cap binding complex) when it itself is in an unphosphorylated state (Showkat, Beigh and Andrabi, 2014). Therefore, mechanistically, initiation factor eIF4E is bound and inactivated by the unphosphorylated translation inhibitor 4E-BP1, but active mTORC1 is able to catalyse the phosphorylation of Thr37/46 of 4E-BP1, which in turn leads to subsequent phosphorylations at Ser65 and Thr70 and the release of the 4E-BP1 from eIF4E, thus enabling eIF4E to fully constitute the cap-binding complex (eIF4F); by its association with the other RNA helicase (eIF4A) and scaffolding protein (eIF4G) subunits. It is the eIF4E subunit, within this trimeric complex, that acts as a mRNA cap-binding protein itself (Gingras *et al.*, 1999). However, the majority of mRNAs do not require active mTOR for their translation, as the amount of available eIF4E is usually sufficient to drive their translational initiation. However, mRNAs containing a 5' UTR TOP-motif are far more sensitive to the amount of available eIF4E due to the inhibitory/ impairing nature of secondary structural motifs often co-associated with the TOP-motif themselves, on the efficiency of translational initiation (Susor *et al.*, 2015). Thus, efficient translation of TOP-motif containing mRNAs requires comparatively elevated levels of free eIF4E than non-TOP-motif containing transcripts, that can be provided by active mTOR mediated phosphorylation of 4EBP1, as shown using the mTOR inhibitor, rapamycin (Dazert and Hall, 2011). The secondary structures occurring in the 5´UTR region in mRNAs containing the TOP motif are known to complicate the translation, even if the exact mechanism by which increased mTOR mediated signalling alleviates this hindrance is not yet fully understood. Accordingly, rapamycin treatment has been shown to result in

decreased levels of phosphorylated of 4E-BP1, and thus shown to increase its affinity for eIF4E, leading to reduced translation of TOP-motif containing mRNAs (Lin *et al.*, 1995; Beretta *et al.*, 1996; von Manteuffel *et al.*, 1996; Gingras, Raught and Sonenberg, 2001).

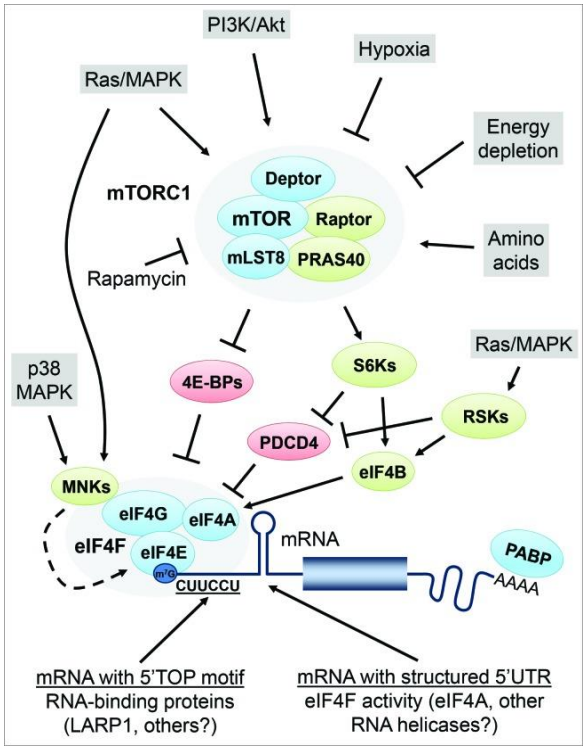

Fig. 7: **Depiction of mTORC1 signalling related to the mechanism of candidate gene translation (Nandagopal and Roux, 2015):** The activity of mTORC1 is stimulated by growth factors/ hormones via the Ras/MAPK and PI3K/Akt signalling pathways to promotes mRNA translation via phosphorylation-dependent regulation of 4E-BPs and S6Ks. Initiation factor eIF4E is occupied by the inhibitory translation factor 4E-BP1, that can then be phosphorylated by the mTORC1 activity to permit effecient translation of mRNAs containing a TOP motif in their 5´UTR.

General mTOR activity is known to be regulated by, amongst other factors, the overall energetic statues of the cell, exposure to specific growth factors signalling molecules (Greene, 1978; Rudkin *et al.*, 1989; Stolovich *et al.*, 2002) amino acid availability (Hay, 2005) and the cell cycle stage (Bass, 2012; Jouffe *et al.*, 2013). Such translational regulation of TOP-motif containing mRNA transcript by mTOR (as described above) has been shown to affect appropriate chromosomal segregation and meiotic spindle positioning in the maturation of mouse oocytes (Susor *et al.*, 2015). Moreover, unpublished findings from our own laboratory have shown that the chemical inhibition of the mTOR pathway (using the inhibitor Torin1), during a short window just prior to and overlapping cell division, negatively influences the generation of ICM founder/ inner cells consequent to the 8- to 16-cell (but curiously, not the 16- to 32-cell) stage transition, during early mouse preimplantation embryonic development (Gahurova et al., manuscript in preparation); potentially via the translational regulation of mRNAs related to spindle orientation/ nuclear position (as reported for oocytes and the extrusion of the first meiotic polar body – (Susor *et al.*, 2015)). In the literature there are a couple of published lists of confirmed and candidate TOP-motif containing mRNAs (based on experimental data and bioinformatic analyses) in the mouse and human genomes (Yamashita *et al.*, 2008; Thoreen *et al.*, 2012); based on such lists we have identified the Dynactin 2 (Dctn2) mRNA (plus other

candidates, such as Ankyrin 2/ Ank2) as a potential mTOR regulated TOP-motif containing transcript involved in the generation of the first inner cells (hypothesised to be biased to ultimately form EPI within the ICM (see above), during the 8- to 16-cell stage transition).

1.5 Dynactin 2

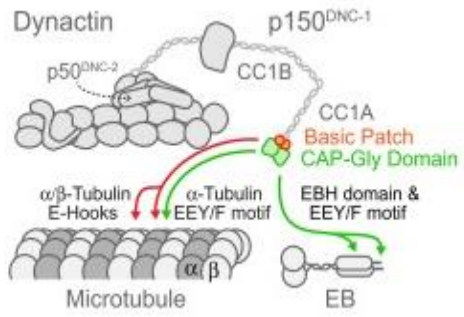

Fig. 8: The interaction between the dynactin complex, microtubules and the end-binding protein (Barbosa *et al.*, 2017): Dctn2 depicated as p50 is the part of the D-D complex side-shoulder and is essential for anchoring microtubules to dynein.

Dctn2 (p50 or dynamitin) is a protein encoded by the gene *Dctn2,* localised on the chromosome 12, as a 50kDa subunit of a dynactin macromolecular complex consisting of 10-11 subunits ranging in size from 22 to 150 kDa. The Dynactin macromolecular complex is connected to microtubules and to cytoplasmic Dynein, the major microtubule minus-end-directed cellular motor, thereby forming the Dynein-Dynactin (D-D) complex. The correct localisation of the D-D complex is essential for a wide range of cellular functions, such as ER-to-Golgi transport, the centripetal movement (movement from Golgi aparatus to the nucleus) of lysosomes and endosomes (Splinter *et al.*, 2012), vesicular transport (Muresan *et al.*, 2001; Kwinter *et al.*, 2009), axonogenesis (Grabham *et al.*, 2007) but also for mitotic spindle formation (Williams *et al.*, 2011) and orientation (Siller and Doe, 2008), chromosome movement and nuclear positioning (Yamamoto *et al.*, 1999, 2001). Dynactin has two important functions associated with its association/ regulation of dynein: (i) the catalytic activation of Dynein that enables it to move along microtubules (Schroer and Sheetz, 1991) and (ii) the binding/ tethering of organelles to Dynein (McGrail *et al.*, 1995; Waterman-Storer *et al.*, 1997), which is crucial for their intra-cellular transport along microtubules. Recruitment of the D-D complex to its cargo is highly dependent on other cofactors, such as Bicaudal D2 (BICD2), which promotes a more stable interaction between Dynactin and Dynein themselves. Moreover, direct and high resolution microscopic visualisation have also shown that the triple D-D-BICD2 complex itself is incompetent to bind microtubules or cargo, whereas tethering of BICD2 to different membranes permits directed motility along microtubules (Splinter *et al.*, 2012). Dctn2 itself is a part of the so-called D-D complex 'side-shoulder' that, together with Dctn1 and Dctn3, plays an important role in anchoring microtubules to Dynein (Fig.8) (Eckley *et al.*, 1999). Dcnt2 can also target the kinetochore

via binding to the constituent zw10 protein and thus potentially plays a role in mitotic spindle checkpoint inactivation, to ensure appropriate segregation of sister chromatids to opposing poles during mitotic cell division (Starr *et al.*, 1998; Howell *et al.*, 2001).

This has been further investigated by analysing the effect of *Dctn2* over-expression on mitosis in vertebrate cells, using immunofluorescence staining of Dynactin and cytoplasmic Dynein components, and has demonstrated that both complexes are recruited to kinetochores within prometaphase and concentrate near the mitotic spindle poles afterwards. The over-expression of Dctn2 in COS-7 cells has been shown to cause interrupted mitosis, with cells arrested in a prometaphase-like state characterised by chromosome condensation spindle contortion and mis-alignment (although the spindles do remain bipolar). As such, these data provide evidence implicating Dynactin (including Dcnt2) and Dynein in roles associated with chromosome alignment and spindle organization (Echeverri *et al.*, 1996). Moreover, the regulatory role of Dctn2 in spindle orientation has been examined in experiments using tissue-specific Integrin-Linked Kinase (ILK) knock-out mice resulting in the disruption of spindle orientation and cell proliferation in intestinal epithelial cells *in vivo*, as ILK together with α-Parvin link Dctn1 and Dctn2 subunits of the D-D complex to Integrin receptors at the basal cortex of mitotic cells. It has been shown that Dctn2 can-not interact with Integrins in the absence of ILK, indicating ILK acts as a linking protein between Integrin receptors and the Dynactin complex, which regulate the mitotic spindle orientation (Morris *et al.*, 2015). It has also been reported that the Dynactin complex has a crucial role in nuclear positioning within post-mitotic *Drosophila melanogaster* photoreceptor neurons. Several experiments based on multiple and functionally independent disruptions of Dynactin complex function have confirmed displacement of the nucleus, such that photoreceptor cells acquired a bipolar appearance with long leading and trailing processes. Moreover, data from this study have also indicated Dynactin as not only cooperating with the microtubule minus end directed motor protein Dynein but also its plus-end directed counterpart, Kinesin. Thus, demonstrating that it is a

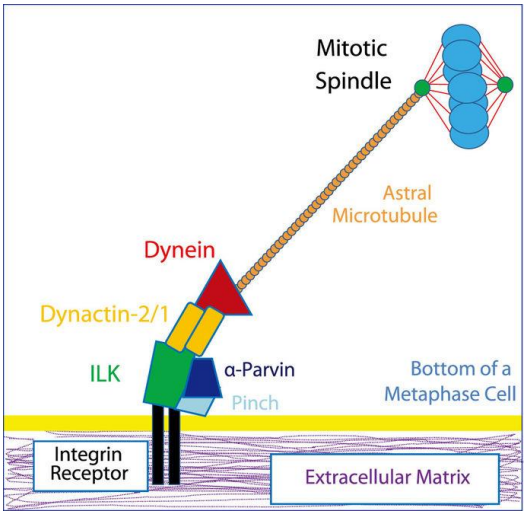

Fig. 9: Schema of the interaction between ILK, Dctn1/2 and Dynein resulting in the regulatory function in spindle orientation closely connected with cell division orientation (Morris *et al.*, 2015).

balance and regulation of these two opposing activities that is essential for the appropriate positioning of the nucleus (Whited, 2004); that could well be relevant to regulating the frequency of asymmetric and symmetric cell cleavage divisions in the early stage mouse embryo (*i.e.* 8- to 16-cell stage transition).

To date, no investigations into the potential role/ mechanism of Dctn2 on spindle orientation and nuclear positioning in the early mouse embryo have been reported. Thus, we wanted to investigate the potential role of Dctn2, as a potential TOP-motif containing and translationally mTOR sensitive mRNA transcript, in spindle orientation and nuclear positioning, during preimplantation embryo development; since it is known that these two factors can affect cell internalisation processes during the first cell fate decision, with potential knock-on consequences for the second cell fate decision in the ICM.

2 Goals of the thesis

1. Dcnt2 presence confirmation in 8- to 16-cell stage embryos

2. Down-regulation of Dctn2 through RNAi

3. Visualisation of the Dctn2 protein in mTOR inhibited and control embryos – Dctn2 primary antibody

4. Visualisation of the Dctn2 protein in control embryos – fluorescently tagged Dctn2 mRNA

3 Materials and methods

3.1 Embryo cultivation

8-9-week old F1 hybrid mouse females (C57Bl6♀×♂CBA/W) were super-ovulated by intra-peritoneal injection of 7.5IU PMSG (pregnant mare serum gonadotrophin extract; Sigma Aldrich) followed by 7.5IU hCG (human chorionic gonadtrophic hormone; Sigma-Aldrich) administered 48 hours later and mated with F1 males. 2-cell stage embryos were recovered into M2 medium containing 4 mg/ml BSA from dissected oviducts approximately 44 hours post hCG administration. The detailed composition of M2 media is shown in table 1.

After washing the embryos through M2 drops covered with mineral oil (Irvine Scientific), they were then either microinjected immediately (see sections 3.3 and 3.4), or washed through KSOM growth media drops (Embyro-Max; Millipore) and cultured in KSOM under mineral oil in a 5% CO_2 containing atmosphere at 37°C until the required stage, either the 8- to 16-cell transition (approximately 32 hours in culture) or 16-cell stage (approximately 40 hours in culture).

When mTOR pathway inhibition was required, the embryos were cultured in KSOM with 200nM Torin1 (Selleckchem), or DMSO (Sigma) vehicle for control, from the mid 8-cell stage (28 hours after the start of the culture) until either the 8- to 16-cell transition (4-8 hours after the start of the Torin1-containing media culture, exact timing was assessed by the embryonic phenotype for the presence of dividing blastomeres) or late 16-cell stage (12 hours after the start of the Torin1/DMSO-containing culture).

Tab. 1: M2 media preparation from concentrated stocks.

STOCK	M2 MEDIA ingred.	g/100ml	TOTAL VOLUME
A (x10)	NaCl	5.534	10.0ml
	KCl	0.356	
	KH2PO4	0.162	
	MgSO4x7H2O	0.293	
	Na-Lactate 60% syrup	3.2(ml)	
	Glucose	1.000	
	Penicilin	0.060	
	Streptomycin	0.050	
B (x10)	NaHCO3	2.101	1.6ml
	Phenol Red	0.010	
C (x100)	Na Pyruvate	3.600	1.0ml
D (x100)	CaCl2x2H2O	2.520	1.0ml
E (x10)	HEPES	5.958	8.4ml
F	BSA		400(mg)
G	H2O		78.0ml

3.2 Microinjections of dsRNA and Venus-tagged mRNA

Beforehand, needle micropipettes, using HARVARD APPARATUS 30-0038 capillaries were prepared using Micropipette Maker machine model PC-10 (Narishige), and holder pipette, using HARVARD APPARATUS 30-0017 capillaries, for the microinjections procedure were prepared. Moreover, plates and pipettes for dissection were prepared (see 3.1). The microinjection apparatus was assembled from 4 parts: i. Fluorescence inverted microscope (OLYMPUS IX71) used for the object observation ii. FemtoJet (positive pressure) microinjection machine (Eppendorf) used for the set-up of the timing, constant pressure and injection pressure iii. Negative capacitance generator (RS Components LtD.) used for the generation of negative capacitance which is necessary for the penetration of the negatively charged phospholipidic embryonic membrane iv. Voltage regulator (WPI) used for current flow visualisation. After the 2-cell stage embryos was dissected one of them were placed on the beforehand prepared stage of the microscope into an M2 drop covered with mineral oil and captured into the holder micropipette. The needle micropipette, in advance loaded with the construct (dsRNA/mRNA), was placed also into the M2 drop as close as possible to the embryo and then either one or both blastomeres of the transferred 2-cell stage embryos were microinjected. The microinjected embryos were further cultivated in KSOM media (see 3.1).

3.3 Fixation, staining, confocal microscopy

3.3.1 Fixation and immunofluorescence staining of the embryos

When embryos reached the required developmental stages the *zona pellucida* was removed by incubation in drops of acid Tyrode's (Sigma). Embryos were fixed in 96-well plates (maximum 15 embryos per well) by 20 minutes incubation at room temperature (RT) in 4% paraformaldehyde (PFA) (Santa Cruz Biotechnology), causing covalent inter-molecular cross-linking, followed by three RT washing steps with 0.15% Tween20 in phosphate buffered saline (PBS), with 20 minutes incubation in the last phosphate buffered saline Tween20 (PBST) wash. Cellular permeabilization was achieved by 20 minutes incubation at RT in 0.5% Triton-X100 (Sigma-Aldrich) diluted in PBS, followed by three washing steps in PBST. Nonspecific epitopes for primary antibody binding were blocked by 30 minutes incubation at 4°C in 3%
bovine serum albumin (BSA) (Sigma-Aldrich) diluted in PBST. Subsequently immuno-staining of Dctn2 protein was performed using an anti-Dctn2 primary antibody

(MyBioSource – cat.n. MBS2522994, raised in rabbit) at a dilution of 1:50 in BSA, in which the embryos were incubated overnight at 4°C. The next day, embryos were washed three times in PBST, incubated for 30 minutes at 4°C in BSA and exposed to an anti-rabbit secondary antibody, conjugated to the Alexa-Fluor555 fluorophore (Life Technologies, cat.n A21429. raised in donkey), at a dilution of 1:500 in BSA for 1 hour in 4°C. This was followed by a PBST washing step and 20 minutes incubation in pure Vectashield (Vector) containing DAPI, for the fluorescent staining of DNA.

Embryos microinjected with fluorescently tagged recombinant Dctn2 mRNA were fixed and washed as described in the previous paragraph, followed by 20 minutes incubation in pure Vectashield (Vector) containing DAPI, without (in most cases) being immuno-stained.

3.3.2 Confocal microscopy

For confocal microscopy imaging a special confocal plate, containing a glass microscope cover slip base (Matek), was prepared with 4 small drops of PBST in which the embryos were placed and scanned on an inverted confocal microscope (Olympus FLUOVIEW FV10i). The appropriate laser excitation and detector emission wave lengths to the secondary antibody conjugated fluorophore and DAPI were selected and each embryo was scanned in its entirety in a series of high-resolution confocal z-sections. Both the percentage of laser power and sensitivity/ gain of the detector were kept constant between all visualised embryos per experiment to enable meaningful signal strength and localisation comparisons, of immuno-fluorescently stained proteins, among different groups of embryos.

3.4 dsRNA preparation and microinjections

3.4.1 Preparation of *Dctn2*specific dsRNA

The preparation of dsRNA specifically targeting murine *Dctn2* derived mRNA transcripts was started with a PCR reaction, serving for the amplification of the desired fragment from a cDNA preparation that would later be used as template in an *in vitro* transcription (IVT) reaction. The cDNA preparation itself was reverse transcribed from RNA previously isolated in the laboratory from mouse testes tissue. The composition of this PCR reaction is shown in table 2 and the primers sequences used (that incorporated T7-RNA polymerase promoter sequences at their 5’ ends) are displayed in table 3. The amplification was performed according to the PCR program illustrated in table 4.

Tab. 2: PCR reaction mix used for Dctn2 dsRNA template preparation (total volume 50 µl).

PCR reaction mix	sample cDNA
Buffer	1x
MgSO4	1.5 mM
dNTPs	0.25 mM
primer S 307	0.30 µM
primer A 307	0.30 µM
cDNA	738 ng
KOD Hot Start DNA Polymerase (Milipore)	1 U

Tab. 3: Primers used for Dctn2 specific dsRNA template generation.

Primers T7_Dctn2		company
primer S 307	TAATACGACTCACTATAGGGGGCATTGCCAGGAATGAG	Sigma-Aldrich
primer A 307	TAATACGACTCACTATAGGGCTGTCCTCTTGGTCTTTCCAA	Sigma-Aldrich

Tab. 4: The PCR program used for Dctn2 specific dsRNA IVT template generation.

PCR program	temperature	time	
denaturation	95°C	2 minutes	
denaturation	95°C	20 seconds	38x
annealing	60°C	10 seconds	
elongation	70°C	10 seconds	
extension	72°C	10 minutes	
cooling	4°C	∞	

The correct size of the PCR product was confirmed by gel electrophoresis in a 1% agarose gel. The amplified template cDNA was then purified by conventional phenol-chloroform organic extraction. Specifically, to the overall 50µl volume of the IVT template DNA, 250µl of HPLC water and 300µl of Tris (pH = 8.0) - saturated phenol were added, vigorously mixed and placed into a 4°C pre-cooled centrifuge and spun for five minutes at 16,000g. The aqueous (upper) phase was transferred into a new 1.5ml Eppendorf tube and 300µl of chloroform was added, similarly mixed, and the centrifugation was repeated as in the previous step. The aqueous phase was pipetted into a new 1.5 ml Eppendorf tube and mixed with a 1/10 volume of 3M NaAc (pH = 5.2), 2.5x volume of 100% ethanol and 2µl of glycogen (concentration = 5mg/ml) and vigorously mixed before being incubated at -20°C overnight, to facilitate DNA precipitation. The next day the sample was centrifuged at

16,000g in 4°C for 30 minutes. After centrifugation, the supernatant was removed, the DNA pellet was washed with 70% ethanol (500µl – 10 minutes 16,000g centrifugation at 4°C) and resuspended in 12µl of nuclease free water. 1µl of the DNA combined with 1µl of water was used for Nanodrop-mediated UV-spectroscopy measurement of concentration and purity and gel electrophoresis for size confirmation analysis.

After confirming the amplified DNA size and concentration, the IVT reaction was assembled and performed using the MEGA Script T7 Kit (Ambion) according to the manufacturer´s instructions. The *in vitro* transcribed dsRNA was purified with phenol-chloroform (in detail described previously in this section; although Tris (pH = 6.7) - saturated phenol was instead used in the initial extraction). Single stranded RNA was removed using specific single-strand RNAse treatment (Invitrogen) according to the manufacturer´s instruction, and the dsRNA was purified by phenol-chloroform extraction and 100% ethanol precipitation, washed twice with 75% ethanol and the resultant purified and air-dried pellet was resuspended in 10µl of nuclease free water. The concentration of the final Dctn2-specific dsRNA was measured by Nanodrop UV-spectroscopy and correct size was confirmed by agarose gel electrophoresis.

dsRNA with a final concentration of 200ng/µl was microinjected (see 3.2) into either one blastomere or both blastomeres of 2-cell stage mouse embryos to elicit either clonal or global down-regulation of *Dctn2* expression (as measure by quantitative RT-PCR analysis of recovered RNA samples, using a C1000 Touch Thermal Cycler from BIO-RAD – see below 3.5.2), respectively.

3.5 mRNA construct preparations and microinjections

3.5.1 Preparation of Venus-*Dctn2* mRNA construct from a IVT plasmid vector

Dctn2 specific mRNA was derived by IVT of a plasmid containing the full-length *Dcnt2* cDNA sequence cloned downstream of a T3 bacteriophage-derived RNA polymerase promotor but upstream of an in-frame cDNA for the Venus fluorescent protein (thus, encoding a C-terminally and fluorescently tagged Dcnt2-Venus fusion gene – cloned in house and described below). The IVT vector used (pRN3-Venus) also ensured the Dcnt2-Venus fusion gene was flanked by both 5´ and 3´ UTR sequences from the frog β-globin gene (designed to provide *in vivo* transcript stability to the IVT derived mRNA construct). Thus, the preparation of the Dcnt2-Venus IVT mRNA construct began with the generation/ cloning of the Dcnt2-Venus IVT compatible plasmid vector, pRN3-Dcnt2-Venus. Accordingly, a PCR reaction consisting of template cDNA (same as in 3.3), utilising the

primers shown in table 6 (designed to incorporate *NheI* restriction enzyme specific recognition sequences at the 5'+3' extremities of the desired product) and the PCR program illustrated in table 7 was performed.

Tab. 5: PCR reaction mix used to generate *Dctn2* cDNA insert (for cloning into pRN3-Venus - total volume 50 µl).

PCR reaction mix	sample cDNA
Buffer	1x
MgSO4	2.50 mM
dNTPs	0.25 mM
primer S 316	0.30 µM
primer A 316	0.30 µM
cDNA	738 ng
KOD Hot Start DNA Polymerase (Milipore)	0.5 U

Tab. 6: Primers used for *Dctn2* cDNA insert generation (for cloning into pRN3-Venus).

Primers Dctn2_CV_		company
primer S 316	GACTATGCTAGCATGGCGGACCCTAAATACGCC	Sigma-Aldrich
primer A 316	GACTATGCTAGCCTTTCCCAGCCTCTTCATCCGA	Sigma-Aldrich

Tab. 7: PCR program used for the amplification of *Dctn2* cDNA insert (for cloning into pRN3-Venus).

PCR program	temperature	time	
denaturation	95°C	2 minutes	
denaturation	95°C	20 seconds	38x
annealing	60°C	10 seconds	
elongation	70°C	2 minutes	
extension	72°C	10 minutes	
cooling	4°C	∞	

The correct size of the PCR product was verified by 1% agarose gel electrophoresis and the remaining product extracted and purified using phenol-chloroform and ethanol precipitation (described in detail in 3.3). Afterwards, the DNA pellet was washed with 70% ethanol and resuspended in 30µl of HPLC water. The amplified Dctn2 cDNA was the digested with 10 units of the restriction enzyme *NheI* (NEBiolabs), in a total volume of 50µl, incubated at 37°C for 3 hours, and purified using a commercial PCR purification Kit (QIAQuick) according to the manufacturer´s instructions. Then the phosphates from the open ends of the vector were removed using Alkaline phosphatase treatment (Roche) to

prevent self-ligation (performed according to the manufacturer´s instructions). The concentration of the purified and *NheI* digested *Dctn2* DNA (*i.e.* the insert) and vector was then measured by Nanodrop mediated UV-spectroscopy and the amount of the insert and vector (pRNA3p) used for ligation was established according to the on-line NEBio calculator (https://nebiocalculator.neb.com/#!/ligation). A DNA ligation reaction was assembled with a ratio of insert to vector of 3:1, in a 20µl total reaction volume, with 1 unit of T4 DNA Ligase (Roche Diagnostics) and incubated in RT for 20 minutes followed by incubation at 4°C for 7 hours (including a control reaction without insert). The ligation product was mixed with competent cells allowing bacteria transformation by heat shock. Specifically, the Eppendorf tube with the mix of competent cells and ligation product was kept on ice for 30 minutes, then transferred into heat block preheated on 42ºC for 90 seconds and then back on ice for 10 minutes. After the transformation of the competent cells, a resuspension (~15µl in residual SOC broth) of the sedimented cells was spread on LB agar plates containing Ampicillin (concentration = 100µg/ml) and incubated at 37ºC overnight. Several bacteria colonies were then streaked out on a new LB agar plate, containing 100µg/ml Ampicillin, in preparation for colony-PCR based screening to confirm successful insertion/ligation of the *Dcnt2* cDNA insert (note that streaking of the colonies is required to minimise the false-positive rate associated with colony-PCR, when performed directly from the initial transformation plate that was spread with a mixture of transformed cells and initial ligation mix). To confirm the presence or absence of the full-length Dctn2 insert in the pRN3-Venus plasmid in each originally picked clone from the initial transformation plate, colony PCR was performed (including positive and negative control) using two different primer combinations (primer sequences can be found in tables 6 and 10) and Taq polymerase in a mastermix (Ampigen). The composition of the PCR mix for colony PCR reactions is illustrated in table 8 and 9. For each colony PCR reaction, a small pipette tip was used to transfer some of the streaked colonies into 9µl of the PCR mix (one colony per reaction). The PCR mix with transformed cells was initially heated to 95°C for 5 minutes to liberate the plasmids from the cells followed by cycling conditions described in table 7 (the same conditions as were used for the amplification of the cDNA template of Venus-tagged Dctn2).

Tab. 8: Colony PCR mix used for full-length insert verification (primer combination 1).

Colony PCR reaction mix	Plasmid DNA
Taq mix	25 µl
primer A 316	0.40 µM
primer T3 frw	0.40 µM
Water	20 µl

Tab. 9: Colony PCR mix used for full-length insert verification (primer combination 2).

Colony PCR reaction mix	Plasmid DNA
Taq mix	25 µl
primer S 316	0.40 µM
primer Venus Reverse	0.40 µM
Water	20 µl

Tab. 10: Primers used for full-length insert verification.

Primers Venus		company
primer Venus Reverse	GACTATTCTAGATCACTTGTACAGCTCGTCCATGCCGAGAGTGA	Sigma-Aldrich
primer T3 frw	GCAATTAACCCTCACTAAAGG	Sigma-Aldrich

Afterwards, plasmids (concentration = 521ng/µl) from the colonies with confirmed *Dcnt2* cDNA inserts (in pRN3-Venus) were isolated and purified using a small-scale commercial plasmid isolation kit (QIAQuick Miniprep - Qiagen), according to the manufacturer's instructions. The purified plasmid concentration was measured by UV spectroscopy on the Nanodrop and the veracity of the *Dcnt2* cDNA insert sequence was confirmed by out-sourced dideoxynucleotide sequencing (NextGEN). 2000ng of the circular plasmid DNA was then digested with 20 units of the restriction enzyme *SfiI* (NEBio), in 20µl total reaction volume, at 50°C for 2 hours. Successful linearization of the plasmid was verified by 0.8% agarose gel electrophoresis (comparing digested and undigested plasmid). The digested plasmid was then purified by phenol-chloroform extraction and ethanol precipitated (as described above). The DNA pellet was resuspended in nuclease free water (10µl) and the concentration was determined by Nanodrop UV spectroscopy (the correct size of the plasmid DNA was further examined by agarose gel electrophoresis). Finally, an IVT reaction using Message Machine T3 Kit (Ambion) was assembled according the

manufacturer´s instructions and mRNA was generated. The newly transcribed Venus-tagged Dctn2 mRNA was than purified by phenol-chloroform extraction and ethanol precipitation (see 3.4.1) and the size of the generated transcript examined on a 0,8 % denaturing agarose gel.

Venus-tagged mRNA with a concentration of 200ng/µl was microinjected into one blastomere of 2-cell stage embryos for clonal over-expression of fluorescently tagged Dctn2 protein.

3.6 Other molecular biology techniques

3.6.1 Confirmation of gene mRNA *Dctn2* down-regulation via QRT PCR

Total RNA was isolated from 16-cell stage Dctn2-knockdown or control embryos that were microinjected at the 2-cell stage with Dctn2-specific or control dsRNA (dsRNA lacking endogenous target, specifically anti-GFP dsRNA) into both blastomeres, using Arcturus Pico Pure RNA Isolation Kit (Thermo Fischer Scientific) according to the manufacturer's instruction. The isolated RNA was treated with 1 unit of DNaseI from the Ambion DNA-free Kit (Invitrogen) followed by inactivation by DNase inactivation reagent (as in manufacturer's instructions). cDNA was then generated by reverse transcription using Superscript III (Invitrogen) and oligo $d(T)_{16}$ primers (Invitrogen) according the manufacturer´s instructions. The generated cDNA was used a template for real-time PCR, employing the SYBR Green PCR kit (Qiagen) using 400nM primers (sequences depicted in table 12 and 13) in 10µl total reaction volumes and as three technical replicates. QRT-PCR was performed using C1000 Touch Thermal Cycler (Biorad) using PCR cycling conditions depicted in table 11. Dctn2 transcript levels were internally normalised against the levels of H2afz , and fold changes attributable to dsRNA, were derived using the ΔΔ Ct method (Livak and Schmittgen, 2001). Melting curves were examined to assess the specificity of the amplification reactions/products.

Tab. 11: QRT PCR program used for KD confirmation.

QRT PCR program	temperature	time	
denaturation	95°C	15 minutes	
denaturation	94°C	25 seconds	39x
annealing	57°C	25 seconds	
elongation	72°C	30seconds	
PLATE READ	/	/	
Melting curves	57°C - 94°C	/	

Tab. 12: Dctn2 primers used for Q-RT-PCR knock-down verification.

Primers QRTPCR Dctn2		company
primer S 315	TCTGGGACCAGATGCTGCAA	Sigma-Aldrich
primer A 315	TCAGGCCGTGAGTGGAGTTC	Sigma-Aldrich

Tab. 13: mH2afz primers used for Q-RT-PCR knock-down verification.

Primers QRTPCR mH2afz		company
primer S 85	GCGCAGCCATCCTGGAGTA	Sigma-Aldrich
primer A 85	CCGATCAGCGATTTGTGGA	Sigma-Aldrich

3.6.2 Confirmation of the presence of Dctn2 mRNA in 16-cell stage mouse embryos

RNA from 16-cell stage embryos, *in vitro* cultured from the 2-cell stage, was extracted and reverse transcribed as described in 3.5.1. The PCR reaction to confirm the presence of Dctn2 mRNA in 16-cell stage embryos was assembled as described in table 14, using cDNA previously prepared from RNA extracted from testis as a positive control. The sequence of primers used for PCR are depicted in table 15 and PCR cycling was performed according to the program illustrated in table 16. The lengths of the PCR products were examined by the 1% agarose gel electrophoresis.

Tab. 14: PCR reaction mix used for Dctn2 presence verification in 16-cell stage mouse embryos (total volume 10 µl).

PCR reaction mix	testis cDNA	16C emryonic cDNA
Buffer	1x	1x
MgSO4	1.50mM	1.50mM
dNTPs	0.05mM	0.05mM
Primer A 307	0.20µM	0.20µM
Primer S 307	0.20µM	0.20µM
Platinum Taq DNA polymerase (Thermo Fischer Scientific)	0.25 U	0.25 U
Examined sample	738 ng	750 ng

Tab. 15: PCR primers used for confirmation of Dcnt2 mRNA expression at the 16-cell stage.

Primers T7_Dctn2		company
primer S 315	TCTGGGACCAGATGCTGCAA	Sigma-Aldrich
primer A 315	TCAGGCCGTGAGTGGAGTTC	Sigma-Aldrich

Tab. 16: PCR program used for confirmation of Dcnt2 mRNA expression at the 16-cell stage.

PCR program	Temperature	Time	
Denaturation	95°C	2 minutes	
Denaturation	95°C	20 seconds	40x
Annealing	62°C	10 seconds	
Elongation	70°C	10 seconds	
Elongation	72°C	10 minutes	
Cooling	4°C	∞	

3.7 Western blotting SDS-PAGE

Torin1-treated and DMSO-treated control embryos (n=60 in each case) were collected at the 16-cell stage (see 3.1), centrifuged at RT for 5 minutes and denatured in lysis buffer containing 1xPBS and 3xSDS-PAGE loading dye (Sodium dodecyl sulfate - SDS, Tris-Cl pH=6.8, Glycerol, Bromophenol blue, β-Mercaptoethanol). Afterwards, the samples were incubated at 97°C for 5 to 7 minutes, so the sample viscosity was diminished and protein denaturation was secured. Western blot apparatus was assembled and filled with 1xSDS running buffer (Tris, Glycine, SDS; pH = 8.3) in which the Triglycin 25% commercial gel (Invitrogen) was placed and all of each protein samples was subsequently loaded, together with the PageRuler Prestained Protein Ladder (TermoFischer Scientific). The gel was run at 90V for approximately 20 minutes until the sample exited the stacking and entered the resolving portion of the gel, when the voltage was increased to 110V for 2 hours. The blotting of the size-resolved proteins from the gel to PVDF membrane was performed using a conventional wet sandwich blotting paper (Whatman) method. The PVDF membrane was first activated by methanol exposure for 40 seconds and subsequent immersion into MilliQ water for 2 minutes. The blotting apparatus was then filled with transfer buffer (Glycine, Tris base, Methanol, ddH_2O; pH = 8.3) and a voltage of 90V passed perpendicularly across the gel-membrane sandwich, allowing the size resolved negatively charged proteins to move towards the positively charged anode and become immobilised onto the PVDF membrane. Thereupon the membrane was placed into a 50ml conical tube with 45ml of dissolved 5% milk powder (diluted in PBST) which was rotated for 1 hour in RT to block out the nonspecific epitopes for primary/secondary antibody binding. The membrane was then probed with anti-Dctn2 primary antibody (MyBioSource) using a 1:5000 dilution (1µl of Dctn2 primary antibody was diluted in 5ml of the 5% milk blocking buffer) by rotating the conical for 2 hours in RT. The blot was then rinsed with three washes of 1xPBST (NaCl,

KCl, Na_2HPO_4, KH_2PO_4, Tween 20 – with pH adjusted to 7.2 and then added ultrapure water), by rotating at RT for 10 minutes. The membrane was then incubated with anti-rabbit secondary antibody (goat anti-Rabbit IgG HRP-conjugate, Biorad, diluted 1:2000 in 5ml of 5% milk blocking buffer), by further rotation for 2 hours in RT. Another PBST washing step followed (as described before) and the membrane was finally rinsed with ECL reagent (Biorad). After this step the membrane was prepared for visualisation and densitometry analysis of revealed immuno-reactive protein bands on a Chemidoc instrument (Biorad) using the ImageLab program. Hereafter, stripping of the PVDF membrane was performed using stripping buffer (Glycine, SDS, Tween20 – with pH adjusted to 2.2 and then added ultrapure water) to remove the primary/secondary antibody and then the probing procedure was repeated with the loading control anti-Hdac1 (Hdac1 is an enzyme regulating eukaryotic gene expression) IgG (Abcam cat.n: ab7028, raised in rabbit) primary antibody diluted 1:1000 in 5% milk and the anti-rabbit secondary antibody (goat anti-Rabbit IgG HRP-conjugate, Biorad) diluted 1:2000 in 5% milk. Visualisation and densitometry analysis followed to normalize the levels of Dctn2 protein.

3.8 Statistical analysis

The statistical analyses were performed using Microsoft Excel. The means and the standard error of means (mean +/- s.e.m) were calculated and statistical significance was determined using two-tailed Student's t-test.

4 Results

4.1 Analysis of the expression level of *Dcnt2* derived mRNA throughout the preimplantation period of mouse embryo development and confirmation of the presence of Dctn2 mRNA in 16-cell stage embryos

It was previously reported, according to the normalised mRNA microarray data obtained by Wang et al 2004, that the expression of *Dctn2* is almost undetectable from fertilisation until 4-cell stage, slightly increases at 8-cell stage and significantly increases at 16-cell stage (illustrated in the figure 10)(Wang *et al.*, 2004). Crucially, this implies an up-regulation of the *Dctn2* expression that is concomitant with the first wave of cell internalisation during mouse embryogenesis (at the 8- to 16-cell transition) and could potentially impinge on the generation of the first ICM founder cells, reported to be ultimately biased to provide progeny that populate the epiblast.

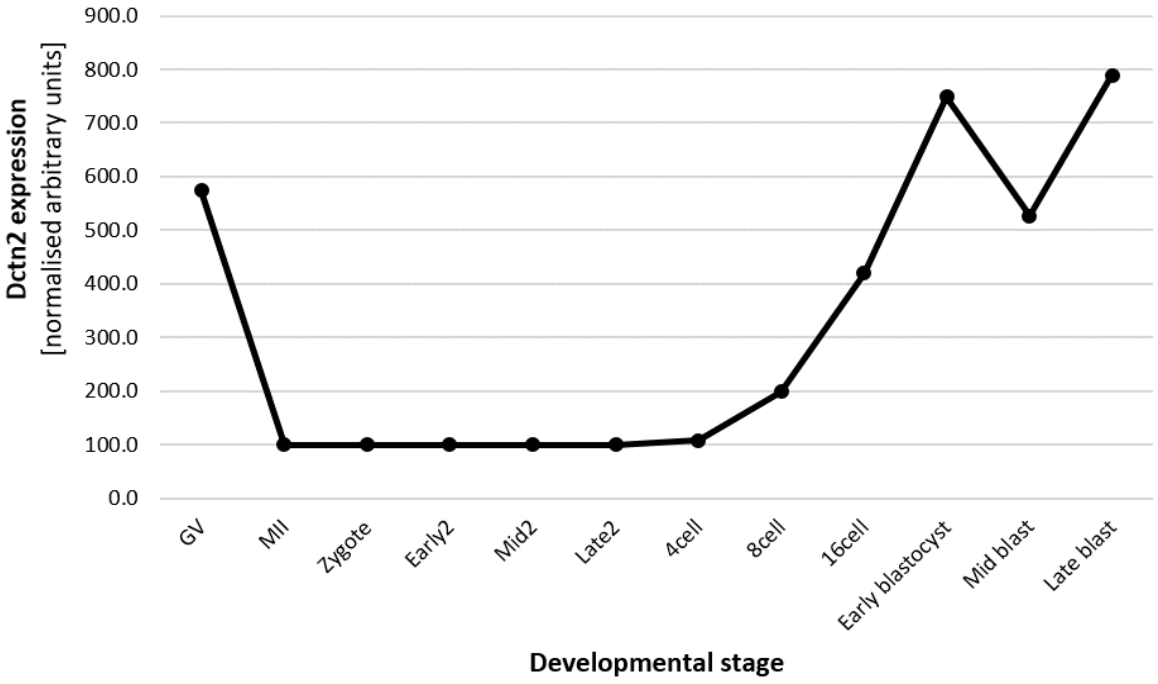

Fig. 10: Chart illustrating the expression of Dctn2 mRNA throughout mouse preimplantation embryonic development (from the germinal vesicle oocyte/GV to late blastocyst/late blast stages) according to Wang *et al.* 2004 mRNA expression microarray data.

The presence of Dctn2 mRNA in 16-cell stage mouse embryos was also confirmed in our own hands by reverse transcription PCR (RT-PCR), followed by gel electrophoresis (see M&M section 3.5.3), using testis cDNA as a positive control. The resulting gel image

(figure 11) confirms that Dctn2 mRNA is present in both testis cDNA and embryonic cDNA samples isolated from 16-cell stage embryos. The size of the PCR products corresponds to the expected size 174 bp. While in the sample with water, used for contamination exclusion, no band was detectable; in the other two samples a clear band of the size 174 bp is detectable, confirming Dcnt2 mRNA expression.

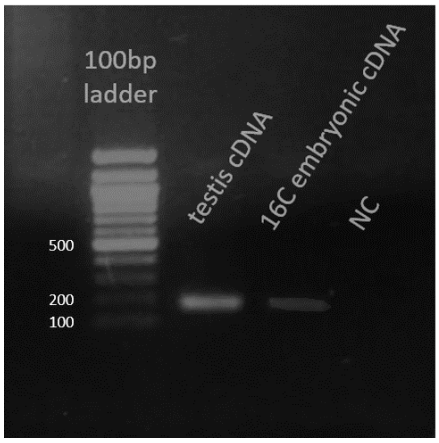

Fig. 11: Agarose gel confirming the presence of Dctn2 mRNA in 16-cell stage embryos. NC indicates negative control.

4.2 *Dctn2* knock-down phenotype

4.2.1 dsRNA preparation specifically targeting Dctn2 mRNA

Dctn2 specific long dsRNA was generated to specifically target the coding sequence of Dctn2 mRNA by RNAi. This was achieved by *in vitro* transcription (IVT) of PCR derived DNA template, itself acquired by amplification of mouse testis cDNA (in detail described in M&M section 3.3.1). The size of the amplified template DNA fragment was examined on the agarose gel depicted in the figure 12. Its size of 248 bp corresponded to the expected size of the band. After this confirmation, the cDNA template of appropriate size was purified and used in IVT to generate dsRNA.

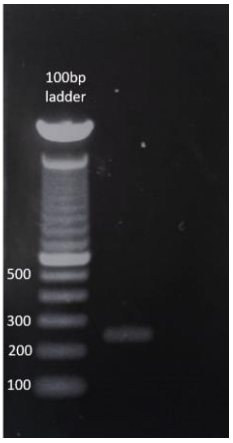

Fig. 12: Agarose gel verifying the size of the amplified cDNA template used for dsRNA generation.

The gel confirming the size of the newly generated and IVT derived dsRNA is depicted in figure 13. Despite the higher concentration of the dsRNA loaded on the gel, the band still clearly corresponds to the expected size of 248bp.

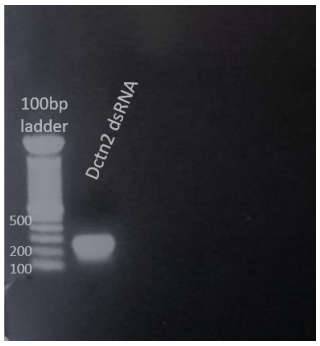

Fig. 13: Final agarose gel verifying the size of the *in vitro* transcribed Dctn2 dsRNA.

4.2.2 Confirmation of Dctn2 down-regulation

Endogenously derived Dctn2 mRNA down-regulation was confirmed by quantitative RT-PCR (QRT-PCR) of 16-cell embryos that had been microinjected with either control (dsRNA lacking endogenous target, specifically anti-GFP dsRNA) or Dcnt2-specific dsRNA into both blastomeres at the 2-cell stage. RNA was isolated from these microinjected controls and Dctn2 knocked-down embryos, reverse transcribed into cDNA and the expression of Dctn2 mRNA was measured by QRT-PCR using Dctn2 specific primers, normalised to the housekeeping gene H2afz. The results are depicted below in the figure 14.

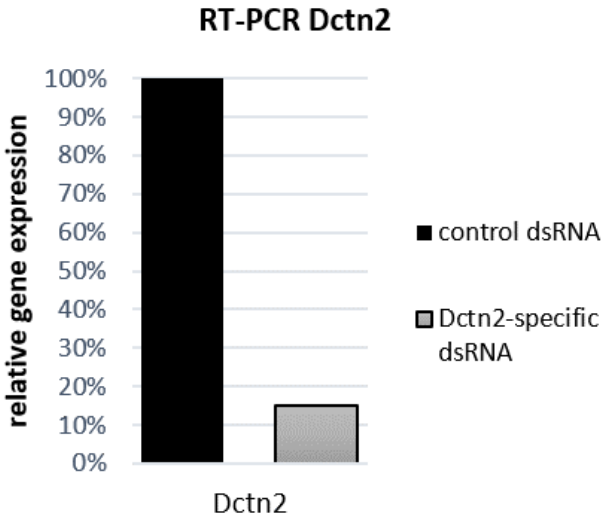

Fig. 14: Bar chart showing the level of Dctn2 mRNA down-regulation caused by Dctn2-specific microinjected dsRNA (relative to Dcnt2 mRNA levels in control dsRNA microinjected embryos, expression values normalised to H2afz gene), using QRT-PCR; thus confirming 85% efficient knockdown in expression.

Figure 14 demonstrates that Dctn2 mRNA expression was decreased in the *Dcnt2*-specific dsRNA microinjected group to 15% of the level observed in control embryos. The knock-down was therefore considered efficient since the expression level of *Dctn2* was reduced by 85%. Thus, by obtaining this result we could be confident that by microinjecting the *Dctn2* specific dsRNA into one blastomere of the 2-cell stage embryo the Dctn2 mRNA expression would be efficiently decreased, in a clonal manner.

4.2.3 The effect of down-regulation of Dctn2 using RNAi

It was hypothesised that clonal knockdown of *Dctn2* expression would affect the normal derivation of inner and outer cells during the 8- to 16-cell stage division, since it was reported that Dctn2 can affect spindle orientation and nuclear position in dividing cells (Whited, 2004; Morris *et al.*, 2015), which thus might affect the generation of the first inner cells during preimplantation mouse embryo development. Specifically, fewer inner cells might be formed from the clone of the Dctn2-specific dsRNA microinjected blastomeres. Therefore, 2-cell stage embryos were dissected and microinjected into one blastomere either with Dctn2 specific dsRNA or with control dsRNA (lacking target in the mouse embryo) mixed together with rhodamine dextran conjugated beads (RBDs) (used as a distinguishing mark between the microinjected and non-microinjected parts/ clones of the embryo) and *in vitro* cultured until the 16-cell stage. The embryos were then fixed and stained with DAPI (staining DNA) and Oregon Green conjugated phalloidin (staining

filamentous F-actin, therefore acting as a marker of cell cortex/ membrane) so that the number of inner/SAD/outer cells could be quantified in the Dctn2 knockdown group and control group of embryos using confocal microscopy. The number of inner and outer, plus so-designated SAD (an abbreviation used to describe outer cells with atypically small apical domains and thus are often apolar and ultimately internalised naturally during the onset of the 16-cell stage (Anani *et al.*, 2014)), cells was compared between the microinjected and non-microinjected parts of the embryo as well as between the knock-down and control group of embryos. The results of the inner/SAD/outer cells analysis are shown in the figure 15.

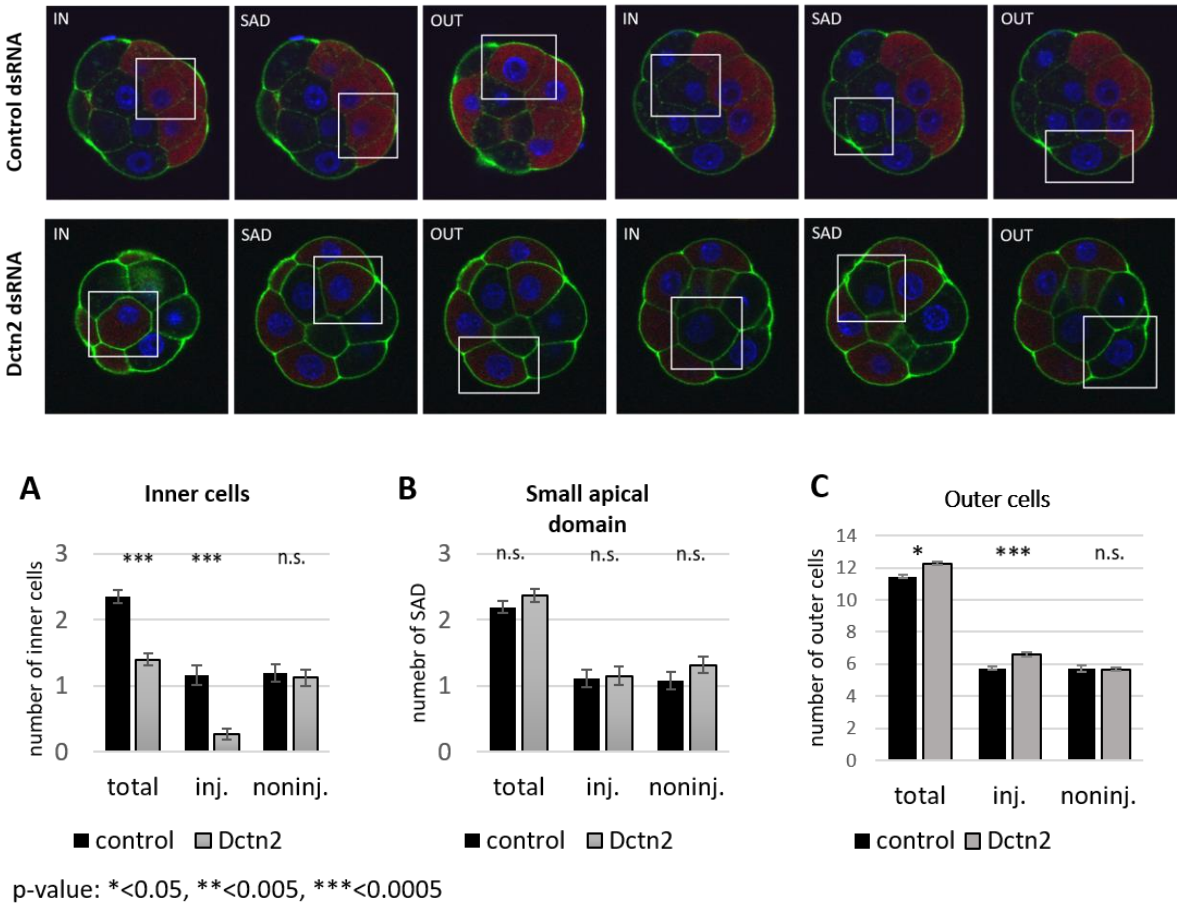

Fig. 15: Statistical analysis of the formation of inner, SAD and outer cells in 16-cell embryos after clonal dsRNA-mediated down-regulation of *Dctn2*.
Chart A: The average number of inner cells formed in embryos microinjected either with control dsRNA or with *Dctn2*-specific dsRNA.
Chart B: Quantification of the average number of outer cells containing a small apical domain (SAD). These cells were counted after microinjections with control or gene-specific dsRNA.
Chart C: Analysis of the average number of outer cell number derived after microinjections of control and gene-specific dsRNA**.**
Control embryo group: n=37, Dcnt2 knock-down experimental group: n = 33

Chart A displays the inner cell number in the two groups of embryos. The first group of embryos marked as control represents embryos microinjected with control dsRNA into one blastomere. The second group marked as Dctn2 refers to embryos microinjected with Dctn2-specific dsRNA targeting Dctn2 mRNA and therefore causes (as confirmed in Fig. 12) a robust down-regulation in the expression of the *Dctn2* gene. In reference to chart A, a highly significant decrease in the average number of total inner cells is observable in the embryos microinjected with Dctn2-specific dsRNA, versus the control dsRNA group (2.3514 ±error 0.0969; 1.3939±error 0.0915). Moreover, this reduction is solely manifested in the reduced average contribution of the *Dcnt2* down-regulated clone of cells (i.e. microinjected with Dctn2 specific dsRNA) as compared to the equivalent clone in control microinjected embryos. The contribution of the progeny of the non-microinjected 2-cell stage blastomere, to the inner cell compartment by the 16-cell stage, was unaffected by microinjection of Dcnt2 dsRNA in the other blastomere. This data demonstrates that the clonal down-regulation of *Dcnt2* expression is associated with a cell-autonomous impairment to contribute to the inner cell compartment by the 16-cell stage. Moreover, that there is no increased and compensatory contribution from the non-microinjected cell clone, acting to regulate the total number of inner cells to levels observed in the control group (at the 16-cell stage), reinforces cell-autonomous nature of the uncovered phenotype. Chart B illustrates the average number of total outer cells per embryo group with a small apical domain (SAD) and the numbers of these SAD outer cells derived from either microinjected or non-microinjected clones. As observed, the total number of SAD cells does not statistically differ between the two investigated groups of embryos with only a slight increase in the *Dcnt2* down-regulated group of embryos, which fails to reach significance. Chart C represents the group of remaining outer cells (*i.e.* not defined as SAD) and describes an opposite trend to that associated with the derivation of inner cells - a statistically significant increase in the total number of non-SAD outer cells in the Dctn2-specific dsRNA microinjected embryos that is accounted for by a robustly significant and increased contribution from the Dcnt2-dsRNA microinjected clone. The number of outer cells in the non-injected halves of embryos in either group remained statistically equivalent. The statistically significant increase of the number of non-SAD outer cells in the embryos clonally injected with *Dctn2*-specific dsRNA reflects and compensates for the statistically significant decrease of the number of inner cells in these embryos (as the total number of cells per assayed embryo was always 16).

The substantial difference between the number of derived inner cells (as a consequence of *Dctn2* down-regulation through RNAi) between the two investigated groups of embryos indicates that *Dctn2* plays an important role during the first cell fate decision, where the nuclear position and spindle orientation might be affected by *Dctn2* gene function. *Dctn2* down-regulation by RNAi affects only the *Dcnt2*-specific dsRNA microinjected clone. On the contrary, microinjected and non-microinjected cells appear to be autonomous as the non-microinjected clones in either group behave equivalently.

4.3 Visualisation of recombinant and fluorescently tagged Dctn2 protein

4.3.1 Preparation of the recombinant Venus-tagged Dcnt2 mRNA

The Venus-tagged Dctn2 mRNA construct was derived from a plasmid (pRN3-Venus) containing the appropriate cDNA (containing a 5' HA-epitope tag) cloned downstream of the T3 bacteriophage-derived RNA polymerase promoter with stabilising 5´ and 3´ UTR sequences from the frog β-globin gene, and a Venus fluorescent protein-coding sequence downstream. During the generation of this pRN3-Venus-Dctn2 construct (performed as part of this project), full-length *Dctn2* insert cDNA was generated by PCR via the amplification of mouse testis cDNA (in detail described in M&M section 3.4.1). The correct size of the amplified *Dctn2* insert cDNA was confirmed by agarose gel electrophoresis (as shown in figure 16) and clearly reports the appropriate and anticipated size of 1257 bp.

Fig. 16: Agarose gel electrophoresis confirming the correct size of the full-length *Dctn2* insert cDNA.

Therefore, the *Dctn2* insert cDNA was subsequently ligated into the pRN3-Venus plasmid vector, transformed (heat shock) into competent cells and cultivated on LB agar plates containing Ampicillin (see M&M section 3.4.1) to select for successful pRN3-Venus-

Dctn2 transformants (screened by colony PCR). Positive colonies were selected for plasmid isolation (via miniprep) and subsequently the veracity of the inserted *Dctn2* cDNA sequence was analysed and confirmed by direct sequencing. A verified pRN3-Venus-Dctn2 plasmid clone was then linearised and used as DNA template in IVT to generate full-length recombinant Venus-tagged Dctn2 mRNA. The size of the newly generated mRNA of approximately 2000 bp (including Dcnt2 and Venus cDNA sequence) was confirmed on the agarose gel depicted in figure 17.

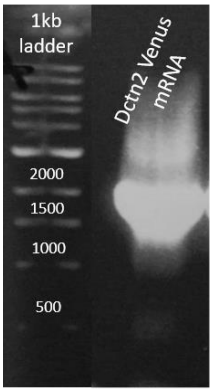

Fig. 17: Full-length Venus-tagged Dctn2 mRNA

4.3.2 Visualisation of the fluorescently tagged Dctn2 protein

Embryos were microinjected (in one blastomere at the 2-cell stage) with fluorescent Venus-tagged Dctn2 mRNA. In addition to the Venus-derived fluorescence of the tagged recombinant Dctn2 protein, the embryos were also immuno-fluorescently (IF) stained with a Dctn2 specific primary antibody to permit fluorescent confocal microscopy mediated visualisation; additionally such IF staining was designed to confirm the specificity of the primary Dctn2 antibody, enabling its subsequent use to probe the expression and subcellular localisation of endogenous Dctn2 in the preimplantation embryo in a reliable manner. The results are illustrated in figure 18.

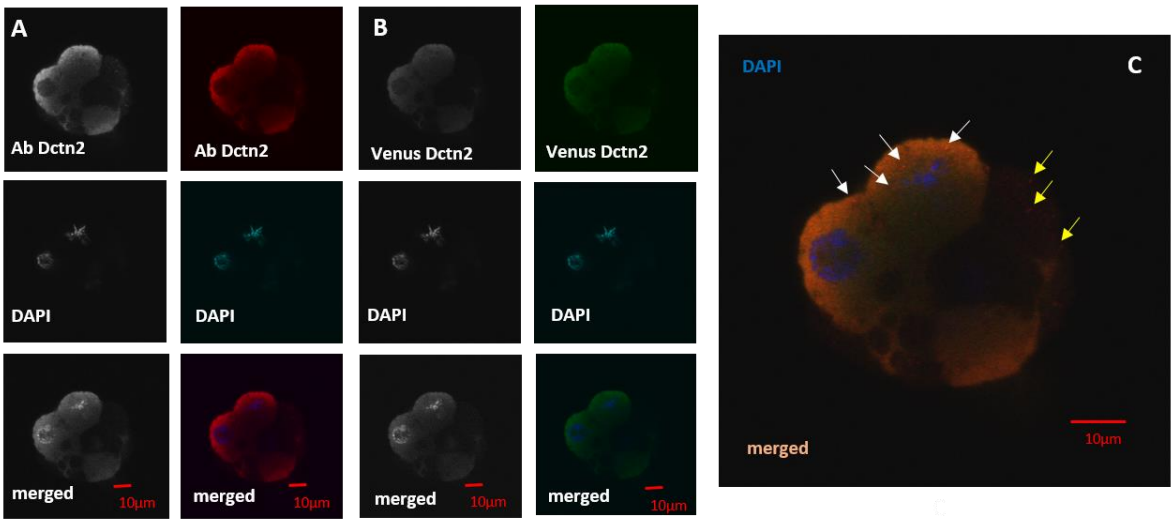

Fig. 18: A representative embryo microinjected with Venus tagged Dctn2 mRNA and IF stained for Dcnt2. Panel **a** shows staining with Dctn2 antibody (shown in greyscale and red, with DNA in greyscale and blue; DAPI), panel **b** shows the inherent fluorescence of recombinant Venus-tagged Dctn2 (shown in greyscale and green, with DNA also in greyscale and blue; DAPI), panel **c** shows an enlarged and merged visualisation of the same embryo. Note, the arrowheads in panel c denote the speckles emerging randomly in the cytoplasm after Dctn2 IF staining in the microinjected (white arrowheads) and non-microinjected (yellow arrowheads) clone.

Figure 18 demonstrates that the microinjection of Venus-tagged Dctn2 mRNA caused the over-expression of recombinant Dcnt2 protein only in the clone originating from originally microinjected 2-cell stage blastomere. It is manifested in the strength of the anti-Dctn2 signal coming from the microinjected clone, compared to the blastomeres originating in the non-microinjected blastomeres. IF staining with the anti-Dctn2 antibody shows co-localisation with the fluorescent signal of the Venus-tagged Dctn2 protein, confirming that the primary anti-Dcnt2 antibody is indeed specific for Dctn2. Also, the Venus-tagged Dctn2 protein localises in the cytoplasm, particularly within cytoplasmic speckles (see arrows; Fig. 18c – merged image) and there is no detectable nuclear signal (see Fig.18a&b). It is noteworthy to highlight that the signal from the recombinant Venus-tagged Dctn2 appears to be brightest in the sub-apical region of outer blastomeres and co-localises with signal from the anti-Dctn2 IF staining; although the comparative reduced IF signal in more internal areas of the blastomeres (including nuclei) may be due to saturation of the primary antibody by recombinant Venus-tagged Dctn2 derived epitopes.

4.4 Torin1 sensitivity

4.4.1 Visualisation of Dctn2 protein in mTOR inhibited and control embryos using a Dctn2 specific primary antibody

It was hypothesised that the translation of Dctn2 mRNA, as it was considered a candidate transcript containing a TOP motif in the 5´UTR region, might be sensitive to mTOR inhibition, using the chemical inhibitor Torin1. Theoretically, Torin1 inhibition during the first wave of cell internalisation, consequent to the 8- to 16-cell transition, might cause a reduction in Dctn2 translation and lead to discernibly lower levels of functional Dctn2 protein. To address this hypothesis, embryos were cultured in parallel under mTOR inhibition conditions using Torin1 and in control conditions using the same concentration of DMSO vehicle control. They were subject to this regime from the mid-8- until the 8- to 16-cell division/ transition, when the first cell fate decision and the first relative spatial allocation of cells occurs, and then fixed for immuno-fluorescent confocal microscopy assaying endogenous Dcnt2 levels; the results are illustrated in figure 19.

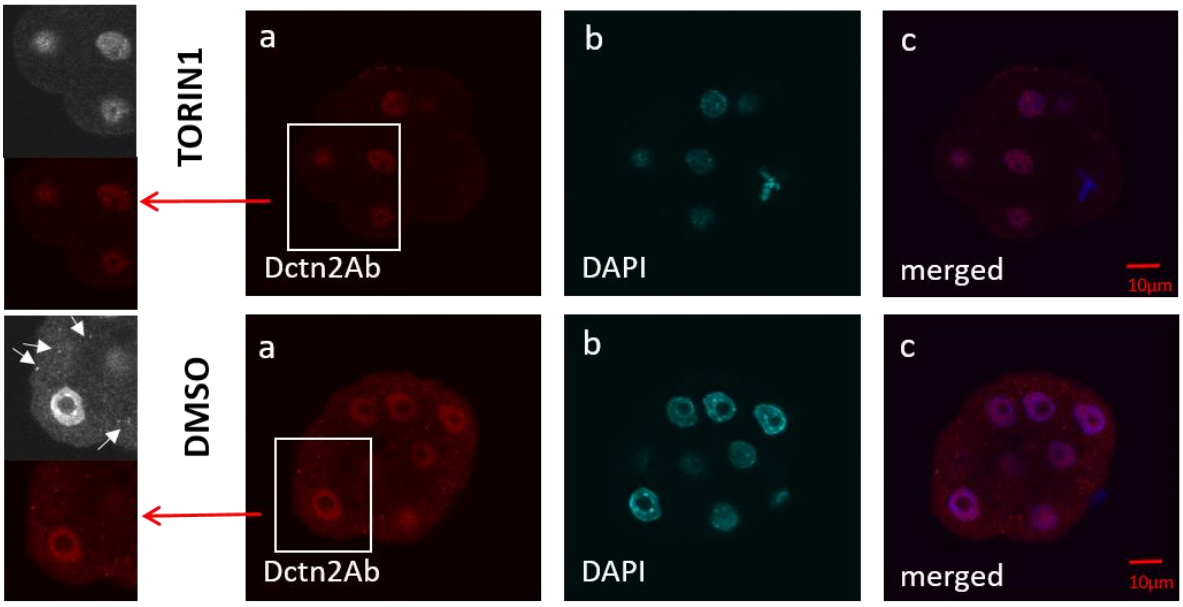

Fig. 19: Illustrative IF staining images of embryos ± mTOR inhibition captured during 8- to 16-cell transition (TORIN1 marks mTOR-inhibited embryos, DMSO marks control embryos). Panel **a** shows staining with a Dctn2 antibody (red), panel **b** shows DNA staining with DAPI (cyan) and merged visualisation is in panel **c** (ref. Methods II.). Magnified insets are shown in both greyscale and pseudo-coloured red for the anti-Dcnt2 IF staining to aid interpretation; arrows denote cytoplasmic speckles of Dcnt2 immuno-reactivity present in control DMSO treated embryos but absent in the Torin1 treated group.

In the control group of embryos Dctn2 is localised in bright cytoplasmic speckles (see arrows in Fig.19a-DMSO - magnified insets) with a lower level of uniform distribution throughout the cytoplasm. In contrast, the mTOR-inhibited embryos exhibit very weak/ basal level of cytoplasmic staining, with a signal that is almost completely absent from any discernible cytoplasmic speckles (see Fig19.a-TORIN1; *n.b.* both illustrative examples were IF stained and image captured using identical confocal microscope settings on the same day). Whereas there is an obvious difference in the amount of cytoplasmic Dctn2 between the two groups, nuclear staining does not appear to change after mTOR inhibition. This nuclear staining was not detectable in the initial characterisation of this primary antibody in embryos microinjected with recombinant Venus-tagged Dctn2 (nor was it observed in the Venus specific channel – see Fig. 18), although this lack of potential endogenous signal could have been due to saturated antibody-recombinant Venus-tagged Dcnt2 interactions in the sub-apical, as stated above. However, subsequent experiments have suggested that this nuclear localised signal is largely an early mouse embryo specific artefact of the fluorescently conjugated secondary antibody used; moreover the fact that the recombinant Venus-tagged Dcnt2 did not localise to the nucleus (as determined by its inherent Venus-derived fluorescence) substantiates this conclusion.

These data strongly suggest that the inhibition of the mTOR pathway, prior to the 8- to 16-cell transition (the first developmental point at which inner/ICM-founder cells can be generated) leads to the down-regulation of Dctn2 protein, located within discreet cytoplasmic speckles, potentially through a mechanism of inhibiting its translation.

4.4.2 Western blotting SDS-PAGE analysis of Dctn2 protein expression in mTOR inhibited and control embryos

The sensitivity to Dctn2 protein levels to Torin1 was further analysed using western blotting SDS-PAGE. Mouse embryos were cultured in parallel under mTOR inhibition conditions using Torin1 and in control conditions using the same concentration of DMSO, as vehicle control, from the mid-8- until the 8- to 16-cell division. Then the Dctn2 protein level in the mTOR-inhibited and control group was determined by western blotting using 60 embryos per sample, and a sample of PMJ2-R macrophages (mouse peritoneal macrophages infected with J2 virus) as a control of the protocol (due to the low amount of input material available from the embryos). Furthermore, anti-Hdac1 (enzyme regulating eukaryotic gene transcript expression) re-probing of the stripped membrane was performed, to serve as a

loading control and a normalising signal for Dctn2 protein expression level determination. The results are depicted in the figure 20.

As we can see in figure 20 (panel A1) the size of the detected anti-Dctn2 bands in both the investigated embryonic groups correspond to 60kDa in contrast to the expected size 45kDa defined by the antibody manufacturer. Interestingly, in the PMJ macrophages samples, two bands were detected - one corresponding to the size of the bands detected in the embryonic samples and another of an approximate size between 40kDa and 55kDa. The single bands detected in the embryonic samples look very clear and we presume that they correspond to the Dctn2 protein that is in someway post-translationally modified and/or multimerised (despite the stringent denaturing/ reducing conditions employed in the protocol). Interestingly, and in keeping with our hypothesis, the intensity of the band in the mTOR-inhibited sample appears to be weaker when compared to the band in the control lane (confirmed by pixel measurements, see below), suggesting there is indeed a lower level of Dctn2 protein expression in 8- to 16-cell stage mouse embryos after mTOR inhibition. The size of the band of the Hdac1 loading control in both the embryonic and PMJ macrophages derived samples corresponds to the expected size of 65 kDa and appeared to be of equal signal intensity; although an additional band of approximately 30 kDa was detected in the macrophage sample (the reason for which remains unclear, but could represent a splice variant or a macrophage unique non-specific interaction).

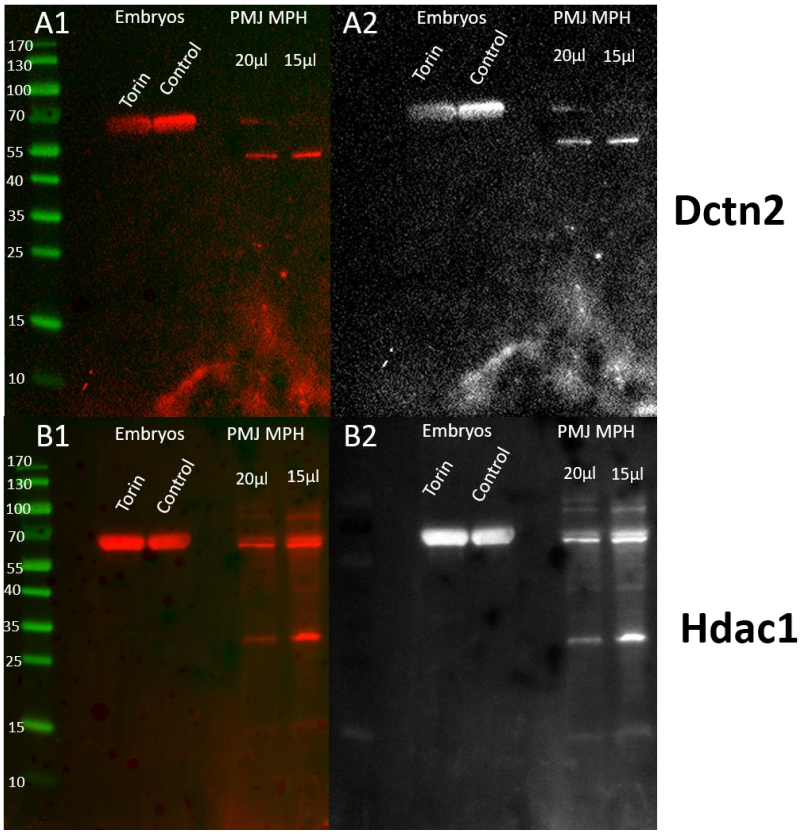

Fig. 20: Western blotting analyses used for the determination of the expression of Dctn2 protein in mTOR-inhibited and control embryos and peritoneal mouse macrophages (PMJ MPH) as a comparison.

A1: Dctn2 protein expression in mTOR-inhibited and control embryos during 8- to 16-cell transition and two different volumes of PMJ macrophage derived protein sample shown in red, ladder shown in green

A2: Dctn2 protein expression in mTOR-inhibited and control embryos during 8- to 16-cell transition and two different volumes of PMJ macrophage derived protein sample shown in greyscale

B1: Hdac1 loading control (used for Dctn2 protein expression normalisation) expression shown in red – western blot membrane re-probed with anti-Hdac1 antibodies after first detecting Dctn2 protein.

B2: Hdac1 loading control (used for Dctn2 protein expression normalisation) expression shown in greyscale – western blot membrane re-probed with anti-Hdac1 antibodies after first detecting Dctn2 protein.

For embryo derived protein samples n=60 embryo equivalents of loaded protein, in each group.

Quantitation of Dctn2 protein expression detected by the above described western blotting was determined using image pixel intensity analysis software (ImageLab program). It was also hypothesised that if mTORC1 regulates the translation of TOP-containing mRNAs including Dctn2, mTOR inhibition would lead to the decreased level of quantified Dctn2 protein expression compared to the levels in control embryos. The results of the analysis are illustrated in the figure 21.

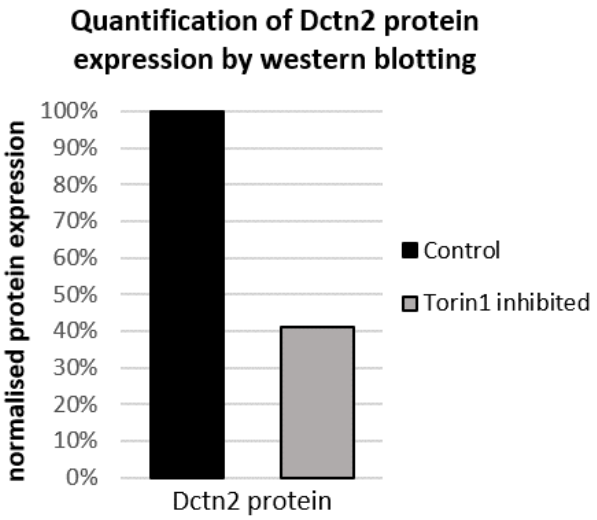

Fig. 21: Relative and normalized (to Hdac1 levels) Dctn2 protein expression levels in control and mTOR-inhibited (by Torin1) embryos; obtained by pixel analysis of the bands detected by western blotting (see Fig. 20).

According to the pixel analysis of the bands representing the Dctn2 protein normalised against those of the Hdac1 loading control, there is a significant decrease in the level of Dctn2 protein expression in the Torin1 treated group of embryos versus the vehicle DMSO control group. The results show that the Dctn2 protein level in Torin1-treated embryos is 41% of the level observed in control embryos. This difference is certainly consistent with our original hypothesis that mTOR inhibition around the time of the generation of the first wave of ICM founders is associated with reduced levels of Dctn2 protein expression (and is in agreement with the same conclusion derived from IF-based assays – see Fig. 19), however, it remains to be verified that the inappropriate size of the observed western blot bands truly correspond to the Dctn2 protein. Hence, other experimental strategies or optimizations need to be devised or addressed (see Discussion).

5 Discussion

The aim of the research conducted within my master´s thesis was to clarify the role of the *Dctn2* gene during mouse preimplantation embryonic development. The described experiments were undertaken based on the fact it is known that Dctn2 has been reported to affect spindle orientation and nuclear positioning (Whited, 2004; Morris *et al.*, 2015), each of which are known to influence the manner in which cells divide that can then, in certain contexts, affect the ultimate cell fate of their generated progeny. Something especially relevant to the spatial segregation of preimplantation stage mouse embryo blastomeres during the first cell-fate decision, from the 8- to 16-cell stage transition. Furthermore, the *Dctn2* gene transcript had been identified as potential candidate mTOR (mTORC1) signalling pathway sensitive mRNA, whose translation is potentially regulated by a putative TOP motif in its 5´ UTR and that could be functionally involved in mediating founder ICM/ inner cell generation (known to be sensitive to mTOR/mTORC1 chemical inhibition – A. W. Bruce lab, unpublished observations). Hence, the expression status of Dctn2 mRNA and protein was investigated and the functional effect (in relation to founder inner cell generation consequent to the 8- to 16-cell transition) determined using a RNAi-based loss-of-function approach; clearly demonstrating a cell-autonomous link between functional Dctn2 expression and inner cell generation in the mouse embryo. Lastly, the sensitivity of Dctn2 protein levels to mTORC1/ mTOR inhibition immediately prior to and encompassing the 8- to 16-cell stage transition was determined to provide evidence that could either support or refute a role for mTOR-mediated control of Dctn2 mRNA translation in supporting the generation of the first founding ICM cells, biased to ultimately populate the pluripotent epiblast, in murine preimplantation stage embryogenesis.

The research was started with experiments focusing on the knock-down of *Dctn2* expression and examining any resulting phenotypes to find out if there would be any significant effect on cell division orientation and the spatial segregation of cells during the 8- to 16-cell stage transition. Taking the data obtained after Dctn2 knock-down into consideration, it was confirmed that the Dctn2 knock-down affects significantly cell division in the manner that less inner cells are generated. The exact mechanistic manner in which this is achieved remains illusive, however, given the fact that Dctn2 is known to affect spindle orientation (Whited, 2004; Morris *et al.*, 2015), one of the crucially important factors effecting the symmetry of cell/blastomere division (Bergstralh, Dawney and St Johnston, 2017), it seems probable that a similar mechanism may operate in the 8-cell stage

blastomeres of dividing mouse embryos; potentially contributing to preferentially align the mitotic spindles parallel to the apico-basal axis (A-B axis), thus resulting in the generation of one outer polarised cell (contributing to TE) and one inner apolar cell (constituting ICM). Moreover, it was hypothesised by Korotkevich et al. that all 8- to 16-cell divisions are in essence asymmetric since it was shown that isolated 8-cell stage blastomeres can be affected to divide asymmetrically by induced polarity (by attaching a bead to one surface) and that the apical domain controls the spindle orientation through microtubule organizing centers (MTOCs). This notion further support our hypothesis that Dctn2 might affect the number of inner cells derived during the 8- to 16-cell division by affecting the spindle orientation, thus less inner cells are generated after Dctn2 knock down implying a requirement of Dctn2 for successful execution of asymmetric divisions. In respect to this hypothesis, it would be interesting to perform Dctn2 global knock down and investigate the acquired phenotype; specifically, how it would impinge on overall inner cell generation. Furthermore, Dctn2 is also known to affect nuclear positioning, another crucially important factor that can define the ultimate symmetry/ orientation of a cell/blastomere division. Indeed, it has been shown in the preimplantation stage embryo that nuclei that are positioned apically, prior to mitotic nuclear envelope breakdown, ultimately and universally give rise to symmetric divisions, resulting in two polarised outer TE-destined daughter cells; moreover, that nearly all asymmetric cell divisions occur as a result of nuclei being positioned to the basolateral portion of the blastomere, although under such circumstances symmetric divisions so still also occur (Ajduk, Biswas Shivhare and Zernicka-Goetz, 2014). Therefore it is equally possible that Dctn2 knock-down could also affect 8-cell stage mouse blastomere nuclear positioning in a manner that ill-favours the generation of inner cells (*i.e*. prevents/ attenuates basolateral nuclear localisation). Whilst, these possibilities only represent speculation, it is highly probable that are other important factors may contribute, either in isolation or in a coordinated manner; for example, mechanical actino-myosin based apical constriction (although we detected no differences in the number of SAD cells generated), transcriptional outputs *etc.*, however, how these would interact with functional Dctn2 remains an open question.

Owing to a paucity of data on the expression status of the *Dctn2* gene, on either the mRNA or protein levels, experiments and analyses were undertaken to investigate *Dctn2* expression within the preimplantation stage embryo. Curiously, analysis of published microarray mRNA expression data (Wang et al., 2004) reported the first expression of the zygotic alleles of the *Dctn2* gene occurring at the 8-cell stage. Given this is the stage at

which pending cell divisions can be either symmetric or asymmetric, resulting in the first spatial segregation of daughter blastomeres with distinct cell-fates, and that our clonal *Dcnt2* knockdown experiments showed a defect in the generation of inner cells during this transition (and not before; *Dctn2* knockdown embryos cultured in step with control microinjected embryos until this stage, with no obvious pre-8-cell stage phenotype), these data argue for an important role for embryo derived Dctn2 protein from the 8-cell stage onwards. Although we did not assay the effect on inner cell generation beyond the 16- cell stage, it would be interesting in the future to see if the phenotype extended to the 16-32 cell transition (the second and last point in preimplantation mouse embryo development inner and outer cells are actively separated); especially given reports in the literature that inner cell generation at this time, particularly after the cell divisions have occurred, is more connected with apical constriction and active cell internalisation (Fierro-González *et al.*, 2013; Samarage *et al.*, 2015; Maître *et al.*, 2016) rather than the orientation of the previous cell division planes (Korotkevich *et al.*, 2017). In an effort to gain a better understanding of the protein expression status of Dctn2 in the preimplantation mouse embryo a full-length Venus-tagged Dctn2 fusion mRNA construct was generated; this was to enable experiments to address the question of the sub-cellular localisation of Dcnt2 protein and to validate the specificity of an acquired anti-Dctn2 antibody in IF studies to reliably detect endogenous protein expression. The expression of the recombinant Venus-tagged Dctn2 indeed did validate the specificity of the antibody to recognised Dcnt2 and helped to demonstrate that the localisation of endogenous Dctn2 at the late 8-cell stage is largely cytoplasmic with randomly distributed brighter speckles (*n.b.* very recently acquired data, in which 8-cell stage blastomeres undergoing mitosis have been captured, has provided evidence for additional Dctn2 localisation on mitotic spindle poles – data not shown). In embryos not expressing recombinant Venus-tagged Dctn2, nuclear staining has also been reliably observed, but considered to be artefactual since it was not affected by mTOR inhibition (unlike the cytoplasmic signals) and nor did the direct recombinant Venus-tagged Dctn2 derived fluorescent signal display any nuclear localisation. Interestingly, the over-expression of Dctn2, when performed in COS-7 cell lines, has been shown to cause interrupted mitosis, with cells arrested in a prometaphase-like state characterised by chromosome condensation, spindle contortion and mis-alignment (although the spindles do remain bipolar) (Echeverri *et al.*, 1996). However, we did not observe any similar phenotypes after Venus-tagged Dctn2 over-expression in mouse embryos. To date, there are not studies reporting the use of a full-length Venus-tagged Dctn2 mRNA in mouse embryos,

as far as referred in reliable sources, but there is evidence about the application of Dctn2 IF staining on research conducted with HeLa cell lines. The pattern of the Dctn2 IF staining performed on HeLa cells profoundly differs being localized exclusively at the basal cell cortex (Morris *et al.*, 2015). Conversely, anti-Dctn2 immuno-staining performed by Echeverri et al., examining the sub-cellular distribution of Dctn2 throughout the cell cycle in cultured mammalian cells, strongly resembles the pattern as described herein within 8-/16- cell stage mouse embryo blastomeres. Specifically, they observed a fine punctate staining densely filling the entire cytoplasm throughout the cell cycle, which was excluded from the nucleus during interphase. Furthermore, they observed a prominent centrosomal staining appearing as a closely spaced group of brighter speckles (compare with our recent data describing mitotic spindle pole localisation – data not shown). Such similarities in this immunostaining patterns bring significant support for the specificity of the anti-Dctn2 primary antibody used in our research, even though, immune-staining was performed on different cells (HeLa, PtK1, COS-7 and Rat2). Because of time constraints, it was not possible to elucidate further the relationship between Dctn2 localisation and its mechanism affecting the generation of inner cells in 16-cell stage mouse embryos. It is important to note that whilst the expression of recombinant Venus-tagged Dctn2 protein in early mouse blastomeres was able to confirm the specificity of the primary anti-Dctn2 antibody used to detect endogenous Dctn2 protein, it remains an open question as to whether the localisation of the Venus-derived fluorescent signal accurately describes the localisation endogenous Dctn2 protein *per se*. This could be because the fusion of the Venus moiety to the Dcnt2 protein could affect other inter-protein interactions required for appropriate sub-cellular localisation (although the Venus signal did also localise to the cytoplasmic speckles identified using the primary anti-Dctn2 antibody in IF).

It was herein hypothesised that the translation of Dctn2, a candidate gene containing a TOP motif in the 5´UTR region, might be regulated by the mTOR signalling pathway. Thus, Dctn2 IF staining on 8- to 16-cell embryos that had formerly been treated with either Torin1 or DMSO vehicle control was performed. While in the embryos treated with DMSO the staining resembled the same pattern as in embryos microinjected with full length Venus-tagged Dctn2 mRNA and stained with Dcnt2 specific primary antibody, the IF staining pattern in the Torin1 inhibited embryos differed. Specifically, the randomly distributed bright speckles disappeared and the cytoplasmic staining appeared to be lower and more uniform after mTOR inhibition. It is important to note that the presented data in each of the two experimental groups (+Torin1 and +DMSO) were obtained in parallel and processed

identically using the same confocal microscope settings, to guard against outside variation contributing to the result. Hence, we are confident in the changes IF staining pattern observed in the +Torin1 groups reflects biological changes associated with mTOR inhibition. To date there are no papers engaged with mTOR inhibition and it´s specific effect on candidate TOP-motif containing gene mRNA translation, such as the *Dctn2* derived transcript investigated here (visualised through IF staining). However, there are some publications concerned with mTOR regulated gene mRNA translation *per se* and general effects of mTOR inhibition on mouse embryos during the preimplantation embryonic developmental period. For instance, Murakami et al. have shown that the disruption of mTOR results in reduced cell size or even leads to embryonic lethality (Murakami *et al.,* 2004). Moreover, similar results were obtained by Gangloff et al. exemplifying that the disruption of the mTOR gene leads to a developmental arrest at E5.5 (Gangloff *et al.,* 2004).

Interestingly, previous examination of mTOR inhibition using Torin1 on mouse oocytes has revealed that this inhibition does not affect significantly spindle formation and function during the first meiosis, and furthermore, that the phosphorylation of the translational inhibitor 4EBP1 is not affected in these oocytes (Severance and Latham, 2017). However, another group has reported the down-regulation of mTOR-regulated translation is associated with spindle abnormalities and problems with chromosomal segregation when the pathway was inhibited by rapamycin, instead of Torin1 (Susor *et al.*, 2015; Jansova *et al.*, 2017). Considering the fact that rapamycin is only capable of affecting the inhibition of mTORC1 alone and Torin1 has the ability to inhibit both mTORC1 and mTORC2, it maybe possible that in the context of the maturing oocyte, inhibition of both complexes masks overt phenotypes that are readily observed when mTORC1 (alone) is inhibited (by rapamycin). However, such masking effect is unlikely to be a factor during the mitotic divisions of the 8- to 16-cell transition in the preimplantation embryo, given that Torin1 based mTOR inhibition gives rise to fewer inner cells (A.W.Bruce – unpublished observations). It would be interesting if the same effect on embryo development (*i.e.* inner cell generation) elicited by Torin1, are also elicited by rapamycin.

The effect of the mTOR signalling pathway on Dctn2 translation was further analysed by western blotting. Although we detected a decrease in the amount of presumed Dctn2 protein after mTOR inhibition, the bands in both embryo groups (±mTOR inhibition) were of a different size to those theoretically expected - approximately 65kDa instead of 45 kDa. PMJ macrophages were used as the experimental control and in these cells two bands

were detected, one matching the band in embryonic samples and one of the expected size 45 kDa. The multiple bands in one lane may be due to distortion effects created by other large bands migrating just above (such as tubulin) or below (such as actin) the Dctn2 specific bands as previously reported in western blotting of Dctn2 performed in studies examining the role of Dctn2 in the appropriate alignment of chromosomes and spindle organisation during mitosis and it´s importance in the modulation of cytoplasmic dynein binding to organelles (Echeverri *et al.*, 1996); albeit to a much lesser extent than we reported here. There are no previous publications referring to western blotting of Dctn2, in any context, after Torin1 inhibition. Potential shortcomings of the methods used here may arise from the denaturation step, where protein dimers/multimers might persist in cases where the sample was not entirely denatured and thus a band containing Dctn2 epitopes of bigger size than expected would theoretically be detected. Alternatively the secondary antibody may be saturated by a different protein (other than Dctn2) binding with a high yet non-specific affinity, however this seems unlike because, the secondary antibody was tested by performing IF staining on the PVFD membrane without former exposure to the Dctn2 specific primary antibody and no signal was detectable (data not shown). Another possible explanation could be the non-specificity of the primary antibody (*i.e.* recognising another, non-Dctn2 protein) or it could be the presence of extensive posttranslational modifications of the Dctn2 protein in the blastomeres of the mouse preimplantation embryo (contributing to its increased migratory retardation in the SDS PAGE gel). Therefore, one option to further account for the anti-Dctn2 primary antibody´s specificity would be elicit global RNAi-based knock-down of Dctn2 expression in the 2-cell stage mouse embryo (by microinjecting the specific dsRNA into both blastomeres) and to repeat western blot, and/or IF-based analyses of the amount of detectable Dctn2 protein expression, that one would predict would be severely diminished (with specific regard to the intensity of 65kDa western blot derived band).

With regard to future aims of my master´s thesis, a Dctn2 TOP motif reporter mRNA construct has been generated, containing an unstable GFP sequence containing the Dctn2 derived TOP motif in 5' UTR. If mTOR regulates translation of TOP-motif containing mRNAs (and specifically Dctn2), mTOR inhibition by Torin1 should lead to a decrease in translation of the construct and therefore decreased GFP fluorescence derived from the microinjected recombinant mRNA. Due to the short stability of GFP, we should be able to precisely map the time window between 8-cell and 16-cell stage when the translation is sensitive to mTOR regulation. Furthermore, an ILK1 (enzyme interacting with many

transmembrane receptors to regulate different signalling cascades) specific primary antibody has also been purchased which might be used for IF co-staining with Dctn2 specific primary antibody. These experiments could eventually reveal more about the localisation of Dctn2 in the mouse embryo at the 8-cell stage (and further in the preimplantation mouse embryonic development) since a paper published by Morris et al. implies an important connection between ILK and Dctn2 as playing an important role in mitotic spindle orientation (Siller and Doe, 2008; Morris *et al.*, 2015). In the context of further expanding our knowledge about the observed phenotype after *Dctn2* knock-down it is scheduled to perform a global knock-down, by microinjections of Dctn2 specific dsRNA into both blastomeres of 2-cell stage embryos, and subsequently quantify the number of inner cells derived at the 16-cell stage; it would be interesting to see if any inner cells would be generated. Additionally, Dctn2 IF staining will also be performed on 16-cell stage embryos globally knocked down by 2-cell stage to analyse if the decrease in the Dctn2 expression would be detected by confocal microscopy (eventually upon further pixel based analysis). Experiments assaying the effect of Dctn2 clonal and global knock-down on inner cell generation at the 16- to 32-cell transition should also be performed.

In conclusion it is important to note that the clarification of the role of the mTOR signalling pathway in inner cell generation and the enlightenment of the exact mechanism, including Dctn2 and the effect of this candidate gene on inner cell generation could be potentially useful for future implications and improvements of *in vitro* fertilisation techniques. Moreover, the furthered understanding of the pattern followed by cells/blastomeres within the crucially important division time-window is on fundamental importance, since it is considered to be an essential requirement for the normal development of the embryo that is still not fully understood.

6 References

Ajduk, A., Biswas Shivhare, S. and Zernicka-Goetz, M. (2014) 'The basal position of nuclei is one pre-requisite for asymmetric cell divisions in the early mouse embryo', *Developmental Biology*. Elsevier, 392(2), pp. 133–140. doi: 10.1016/j.ydbio.2014.05.009.

Anani, S. *et al.* (2014) 'Initiation of Hippo signaling is linked to polarity rather than to cell position in the pre-implantation mouse embryo', *Development*, 141(14), pp. 2813–2824. doi: 10.1242/dev.107276.

Artus, J. and Cohen-Tannoudji, M. (2008) 'Cell cycle regulation during early mouse embryogenesis', *Molecular and Cellular Endocrinology*. Elsevier, 282(1–2), pp. 78–86. doi: 10.1016/J.MCE.2007.11.008.

Avilion, A. A. *et al.* (2003) 'Multipotent cell lineages in early mouse development on SOX2 function', *Genes Dev.*, 17, pp. 126–140. doi: 10.1101/gad.224503.

Barbosa, D. J. *et al.* (2017) *Dynactin binding to tyrosinated microtubules promotes centrosome centration in C . elegans by enhancing dynein-mediated organelle transport*.

Bass, J. (2012) 'Circadian topology of metabolism', *Nature*. Nature Publishing Group, pp. 348–356. doi: 10.1038/nature11704.

Beck, F. *et al.* (2003) 'A study of regional gut endoderm potency by analysis of Cdx2 null mutant chimaeric mice', *Developmental Biology*. Academic Press, 255(2), pp. 399–406. doi: 10.1016/S0012-1606(02)00096-9.

Beretta, L. *et al.* (1996) 'Rapamycin blocks the phosphorylation of 4E-BP1 and inhibits cap-dependent initiation of translation.', *The EMBO journal*, 15(3), pp. 658–664. doi: 10.1002/J.1460-2075.1996.TB00398.X.

Bergstralh, D. T., Dawney, N. S. and St Johnston, D. (2017) 'Spindle orientation: a question of complex positioning.', *Development (Cambridge, England)*. Oxford University Press for The Company of Biologists Limited, 144(7), pp. 1137–1145. doi: 10.1242/dev.140764.

Bessonnard, S. *et al.* (2017) 'ICM conversion to epiblast by FGF/ERK inhibition is limited in time and requires transcription and protein degradation', *Scientific Reports*, 7(1), p. 12285. doi: 10.1038/s41598-017-12120-0.

Bruce, A. W. and Zernicka-Goetz, M. (2010) 'Developmental control of the early mammalian embryo: competition among heterogeneous cells that biases cell fate', *Current Opinion in Genetics & Development*. Elsevier Current Trends, 20(5), pp. 485–491. doi: 10.1016/J.GDE.2010.05.006.

Bulut-Karslioglu, A. *et al.* (2016) 'Inhibition of mTOR induces a paused pluripotent state', *Nature*. Nature Publishing Group, 540(7631), pp. 119–123. doi: 10.1038/nature20578.

Burnett, P. E. *et al.* (1998) 'RAFT1 phosphorylation of the translational regulators p70 S6 kinase and 4E-BP1', *Proceedings of the National Academy of Sciences*. National Academy of Sciences, 95(4), pp. 1432–1437. doi: 10.1073/pnas.95.4.1432.

Chambers, I. *et al.* (2003) 'Functional Expression Cloning of Nanog, a Pluripotency Sustaining Factor in Embryonic Stem Cells', *Cell*. Cell Press, 113(5), pp. 643–655. doi: 10.1016/S0092-8674(03)00392-1.

Chazaud, C. *et al.* (2006) 'Early Lineage Segregation between Epiblast and Primitive Endoderm in Mouse Blastocysts through the Grb2-MAPK Pathway', *Developmental Cell*. Cell Press, 10(5), pp. 615–624. doi: 10.1016/j.devcel.2006.02.020.

Cockburn, K. and Rossant, J. (2010) 'Making the blastocyst: Lessons from the mouse', *Journal of Clinical Investigation*, 120(4), pp. 995–1003. doi: 10.1172/JCI41229.

Codogno, P. and Meijer, A. J. (2005) 'Autophagy and signaling: their role in cell survival and cell death', *Cell Death Differ*. Nature Publishing Group, 12 Suppl 2(S2), pp. 1509–1518. doi: 4401751 [pii]\n10.1038/sj.cdd.4401751.

Dard, N. *et al.* (2008) 'Morphogenesis of the mammalian blastocyst', *Molecular and Cellular Endocrinology*. Elsevier, 282(1–2), pp. 70–77. doi: 10.1016/J.MCE.2007.11.004.

Dard, N., Louvet-Vallée, S. and Maro, B. (2009) 'Orientation of mitotic spindles during the 8- to 16-cell stage transition in mouse embryos', *PLoS ONE*, 4(12), pp. 6–13. doi: 10.1371/journal.pone.0008171.

Dazert, E. and Hall, M. N. (2011) 'MTOR signaling in disease', *Current Opinion in Cell Biology*. Elsevier Current Trends, pp. 744–755. doi: 10.1016/j.ceb.2011.09.003.

Echeverri, C. J. *et al.* (1996) 'Molecular characterization of the 50-kD subunit of dynactin reveals function for the complex in chromosome alignment and spindle organization during mitosis', *Journal of Cell Biology*, 132(4), pp. 617–633. doi: 10.1083/jcb.132.4.617.

Eckert, J. J. *et al.* (2004) 'Specific PKC isoforms regulate blastocoel formation during mouse preimplantation development', *Developmental Biology*. Academic Press, 274(2), pp. 384–401. doi: 10.1016/J.YDBIO.2004.07.027.

Eckley, D. M. *et al.* (1999) 'Analysis of dynactin subcomplexes reveals a novel actin-related protein associated with the Arp1 minifilament pointed end', *Journal of Cell Biology*, 147(2), pp. 307–319. doi: 10.1083/jcb.147.2.307.

Fadden, P., Haystead, T. A. and Lawrence, J. C. (1997) 'Identification of phosphorylation sites in the translational regulator, PHAS-I, that are controlled by insulin and rapamycin in rat adipocytes.', *The Journal of biological chemistry*. American Society for Biochemistry and Molecular Biology, 272(15), pp. 10240–7. doi: 10.1074/JBC.272.15.10240.

Fierro-González, J. C. *et al.* (2013) 'Cadherin-dependent filopodia control preimplantation embryo compaction', *Nature Cell Biology*. Nature Publishing Group, 15(12), pp. 1424–1433. doi: 10.1038/ncb2875.

Frankenberg, S. *et al.* (2011) 'Primitive Endoderm Differentiates via a Three-Step Mechanism Involving Nanog and RTK Signaling', *Developmental Cell*. Cell Press, 21(6), pp. 1005–1013. doi: 10.1016/J.DEVCEL.2011.10.019.

Gangloff, Y.-G. *et al.* (2004) 'Disruption of the Mouse mTOR Gene Leads to Early Postimplantation Lethality and Prohibits Embryonic Stem Cell Development', *Molecular and Cellular Biology*. American Society for Microbiology, 24(21), pp. 9508–9516. doi: 10.1128/MCB.24.21.9508-9516.2004.

Gingras, A. C. *et al.* (1999) 'Regulation of 4E-BP1 phosphorylation: a novel two-step mechanism.', *Genes & development*. Cold Spring Harbor Laboratory Press, 13(11), pp. 1422–37. Available at: http://www.ncbi.nlm.nih.gov/pubmed/10364159 (Accessed: 28 February 2018).

Gingras, A. C., Raught, B. and Sonenberg, N. (2001) 'Regulation of translation initiation by FRAP/mTOR', *Genes and Development*. Cold Spring Harbor Laboratory Press, pp. 807–826. doi: 10.1101/gad.887201.

Grabham, P. W. *et al.* (2007) 'Cytoplasmic Dynein and LIS1 Are Required for Microtubule Advance during Growth Cone Remodeling and Fast Axonal Outgrowth', *Journal of Neuroscience*, 27(21), pp. 5823–5834. doi: 10.1523/JNEUROSCI.1135-07.2007.

Greene, L. A. (1978) 'Nerve growth factor prevents the death and stimulates the neuronal differentiation of clonal PC12 pheochromocytoma cells in serum-free medium', *Journal of Cell Biology*. Rockefeller University Press, 78(3), pp. 747–755. doi: 10.1083/jcb.78.3.747.

Guertin, D. A. and Sabatini, D. M. (2007) 'Defining the Role of mTOR in Cancer', *Cancer Cell*. Cell Press, pp. 9–22. doi: 10.1016/j.ccr.2007.05.008.

Hamilton, T. L. *et al.* (2006) 'TOPs and their regulation', *Biochemical Society Transactions*. Portland Press Limited, 34(1), p. 12. doi: 10.1042/BST20060012.

Hay, N. (2005) 'The Akt-mTOR tango and its relevance to cancer', *Cancer Cell*. Cell Press, pp. 179–183. doi: 10.1016/j.ccr.2005.08.008.

Howell, B. J. *et al.* (2001) 'Cytoplasmic dynein/dynactin drives kinetochore protein transport to the spindle poles and has a role in mitotic spindle checkpoint inactivation', *Journal of Cell Biology*. The Rockefeller University Press, 155(7), pp. 1159–1172. doi: 10.1083/jcb.200105093.

Jansova, D. *et al.* (2017) 'Regulation of 4E-BP1 activity in the mammalian oocyte', *Cell Cycle*. Taylor & Francis, 16(10), pp. 927–939. doi: 10.1080/15384101.2017.1295178.

Jedrusik, A. *et al.* (2008) 'Role of Cdx2 and cell polarity in cell allocation and specification of trophectoderm and inner cell mass in the mouse embryo.', *Genes & development*. Cold Spring Harbor Laboratory Press, 22(19), pp. 2692–706. doi: 10.1101/gad.486108.

Johnson, M. H. (2009) 'From Mouse Egg to Mouse Embryo: Polarities, Axes, and Tissues', *Annual Review of Cell and Developmental Biology*, 25(1), pp. 483–512. doi: 10.1146/annurev.cellbio.042308.113348.

Johnson, M. H. and Ziomek, C. A. (1983) 'Cell interactions influence the fate of mouse blastomeres undergoing the transition from the 16- to the 32-cell stage', *Developmental Biology*. Academic Press, 95(1), pp. 211–218. doi: 10.1016/0012-1606(83)90019-2.

Jouffe, C. *et al.* (2013) 'The Circadian Clock Coordinates Ribosome Biogenesis', *PLoS Biology*. Edited by P. E. Hardin. Public Library of Science, 11(1), p. e1001455. doi: 10.1371/journal.pbio.1001455.

Kang, J., Nachtrab, G. and Poss, K. D. (2013) 'Local Dkk1 Crosstalk from Breeding Ornaments Impedes Regeneration of Injured Male Zebrafish Fins', *Developmental Cell*, 27(1), pp. 19–31. doi: 10.1016/j.devcel.2013.08.015.

Kang, M. *et al.* (2013) 'FGF4 is required for lineage restriction and salt-and-pepper distribution of primitive endoderm factors but not their initial expression in the mouse', *Development*, 140(2), pp. 267–279. doi: 10.1242/dev.084996.

Kelly, S. J. (1977) 'Studies of the developmental potential of 4- and 8-cell stage mouse blastomeres', *Journal of Experimental Zoology*, 200(3), pp. 365–376. doi: 10.1002/jez.1402000307.

Kim, J. E. and Chen, J. (2004) 'Regulation of peroxisome proliferator-activated receptor-?? activity by mammalian target of rapamycin and amino acids in adipogenesis', *Diabetes*, 53(11), pp. 2748–2756. doi: 10.2337/diabetes.53.11.2748.

Korotkevich, E. *et al.* (2017) 'The Apical Domain Is Required and Sufficient for the First Lineage Segregation in the Mouse Embryo', *Developmental Cell*, 40(3), p. 235–247.e7. doi: 10.1016/j.devcel.2017.01.006.

Krupa, M. *et al.* (2014) 'Allocation of inner cells to epiblast vs primitive endoderm in the mouse embryo is biased but not determined by the round of asymmetric divisions (8→16- and 16→32-cells)', *Developmental Biology*. Academic Press, 385(1), pp. 136–148. doi: 10.1016/J.YDBIO.2013.09.008.

Kwinter, D. M. *et al.* (2009) 'Dynactin regulates bidirectional transport of dense-core vesicles in the axon and dendrites of cultured hippocampal neurons', *Neuroscience*. Pergamon, 162(4), pp. 1001–1010. doi: 10.1016/J.NEUROSCIENCE.2009.05.038.

Laplante, M. and Sabatini, D. M. (2009) 'mTOR signaling at a glance.', *Journal of cell science*. The Company of Biologists Ltd, 122(Pt 20), pp. 3589–94. doi: 10.1242/jcs.051011.

Lin, T. A. *et al.* (1994) 'PHAS-I as a link between mitogen-activated protein kinase and translation initiation.', *Science (New York, N.Y.)*. American Association for the Advancement of Science, 266(5185), pp. 653–6. doi: 10.1126/SCIENCE.7939721.

Lin, T. A. *et al.* (1995) 'Control of PHAS-I by insulin in 3T3-L1 adipocytes: Synthesis, degradation, and phosphorylation by a rapamycin-sensitive and mitogen-activated protein kinase-independent pathway', *Journal of Biological Chemistry*. American Society for Biochemistry and Molecular Biology, 270(31), pp. 18531–18538. doi: 10.1074/jbc.270.31.18531.

Livak, K. J. and Schmittgen, T. D. (2001) 'Analysis of relative gene expression data using real-time quantitative PCR and', *Methods*. Academic Press, 25(4), pp. 402–408. doi: 10.1006/meth.2001.1262.

Ma, X. M. and Blenis, J. (2009) 'Molecular mechanisms of mTOR-mediated translational control', *Nature Reviews Molecular Cell Biology*. Nature Publishing Group, pp. 307–318. doi: 10.1038/nrm2672.

Maître, J.-L. *et al.* (2016) 'Asymmetric division of contractile domains couples cell positioning and fate specification', *Nature*. Nature Publishing Group, 536(7616), pp. 344–348. doi: 10.1038/nature18958.

Mansour, A. A. and Hanna, J. H. (2013) 'Oct4 shuffles Sox partners to direct cell fate.', *The EMBO journal*. European Molecular Biology Organization, 32(7), pp. 917–9. doi: 10.1038/emboj.2013.48.

von Manteuffel, S. R. *et al.* (1996) '4E-BP1 phosphorylation is mediated by the FRAP-p70s6k pathway and is independent of mitogen-activated protein kinase.', *Proceedings of the National Academy of Sciences of the United States of America*, 93(9), pp. 4076–80. doi: 10.1073/pnas.93.9.4076.

Marikawa, Y. and Alarcón, V. B. (2009) 'Establishment of trophectoderm and inner cell mass lineages in the mouse embryo', *Molecular Reproduction and Development*, 76(11), pp. 1019–1032. doi: 10.1002/mrd.21057.

McGrail, M. *et al.* (1995) 'Regulation of cytoplasmic dynein function in vivo by the Drosophila glued complex', *Journal of Cell Biology*. Rockefeller University Press, 131(2), pp. 411–425. doi: 10.1083/jcb.131.2.411.

Meyuhas, O. and Kahan, T. (2015) 'The race to decipher the top secrets of TOP mRNAs', *Biochimica et Biophysica Acta - Gene Regulatory Mechanisms*. Elsevier, pp. 801–811. doi: 10.1016/j.bbagrm.2014.08.015.

Mihajlović, A. I. and Bruce, A. W. (2017) 'The first cell-fate decision of mouse preimplantation embryo development: integrating cell position and polarity', *Open Biology*. Royal Society Journals, 7(11), p. 170210. doi: 10.1098/rsob.170210.

Mihajlović, A. I., Thamodaran, V. and Bruce, A. W. (2015) 'The first two cell-fate decisions of preimplantation mouse embryo development are not functionally independent', *Scientific Reports*. Nature Publishing Group, 5, p. 15034. doi: 10.1038/srep15034.

Mitsui, K. *et al.* (2003) 'The Homeoprotein Nanog Is Required for Maintenance of Pluripotency in Mouse Epiblast and ES Cells', *Cell*. Cell Press, 113(5), pp. 631–642. doi: 10.1016/S0092-8674(03)00393-3.

Morris, E. J. *et al.* (2015) 'Integrin-Linked Kinase links Dynactin-1/Dynactin-2 with cortical Integrin receptors to orient the mitotic spindle relative to the substratum', *Scientific Reports*. Nature Publishing Group, 5(1), p. 8389. doi: 10.1038/srep08389.

Morris, S. A. *et al.* (2010) 'Origin and formation of the first two distinct cell types of the inner cell mass in the mouse embryo', *Proc Natl Acad Sci U S A*, 107(14), pp. 6364–6369. doi: 10.1073/pnas.0915063107.

Morris, S. A. *et al.* (2013) 'The differential response to Fgf signalling in cells internalized at different times influences lineage segregation in preimplantation mouse embryos', *Open Biology*, 3(11), pp. 130104–130104. doi: 10.1098/rsob.130104.

Morris, S. A. A., Guo, Y. and Zernicka-Goetz, M. (2012) 'Developmental Plasticity Is Bound by Pluripotency and the Fgf and Wnt Signaling Pathways', *Cell Reports*. The Authors, 2(4), pp. 756–765. doi: 10.1016/j.celrep.2012.08.029.

Murakami, M. *et al.* (2004) 'mTOR is essential for growth and proliferation in early mouse embryos and embryonic stem cells.', *Molecular and cellular biology*. American Society for Microbiology, 24(15), pp. 6710–8. doi: 10.1128/MCB.24.15.6710-6718.2004.

Muresan, V. *et al.* (2001) 'Dynactin-Dependent, Dynein-Driven Vesicle Transport in the Absence of Membrane Proteins: A Role for Spectrin and Acidic Phospholipids', *Molecular Cell*. Cell Press, 7(1), pp. 173–183. doi: 10.1016/S1097-2765(01)00165-4.

Nandagopal, N. and Roux, P. P. (2015) 'Regulation of global and specific mRNA translation by the mTOR signaling pathway', *Translation*, 3(1), p. e983402. doi: 10.4161/21690731.2014.983402.

Nichols, J. *et al.* (2009) 'Suppression of Erk signalling promotes ground state pluripotency in the mouse embryo.', *Development (Cambridge, England)*. The Company of Biologists Ltd, 136(19), pp. 3215–22. doi: 10.1242/dev.038893.

Nishioka, N. *et al.* (2008) 'Tead4 is required for specification of trophectoderm in pre-implantation mouse embryos', *Mechanisms of Development*. Elsevier, 125(3–4), pp. 270–283. doi: 10.1016/J.MOD.2007.11.002.

Niwa, H. *et al.* (2005) 'Interaction between Oct3/4 and Cdx2 determines trophectoderm differentiation', *Cell*. Cell Press, 123(5), pp. 917–929. doi: 10.1016/j.cell.2005.08.040.

Paria, B. C. and Dey, S. K. (1990) 'Preimplantation embryo development in vitro: cooperative interactions among embryos and role of growth factors.', *Proceedings of the National Academy of Sciences of the United States of America*. National Academy of Sciences, 87(12), pp. 4756–60. doi: 10.1073/PNAS.87.12.4756.

Pause, A. *et al.* (1994) 'Insulin-dependent stimulation of protein synthesis by phosphorylation of a regulator of 5'-cap function', *Nature*. Nature Publishing Group, 371(6500), pp. 762–767. doi: 10.1038/371762a0.

Piotrowska-Nitsche, K. and Zernicka-Goetz, M. (2005) 'Spatial arrangement of individual 4-cell stage blastomeres and the order in which they are generated correlate with blastocyst pattern in the mouse embryo', *Mechanisms of Development*, 122(4), pp. 487–500. doi: 10.1016/j.mod.2004.11.014.

Richter, J. D. and Sonenberg, N. (2005) 'Regulation of cap-dependent translation by eIF4E inhibitory proteins', *Nature*. Nature Publishing Group, 433(7025), pp. 477–480. doi: 10.1038/nature03205.

Rossant, J. (1976) 'Postimplantation development of blastomeres isolated from 4- and 8-cell mouse eggs.', *Journal of embryology and experimental morphology*, 36(2), pp. 283–90. Available at: http://www.ncbi.nlm.nih.gov/pubmed/1033982.

Rudkin, B. B. *et al.* (1989) 'Cell cycle-specific action of nerve growth factor in PC12 cells : differentiation without proliferation', *The EMBO Journal*, 8(1), pp. 3319–3325. doi: 10.1002/j.1460-2075.1989.tb08493.x.

Russ, A. P. *et al.* (2000) 'Eomesodermin is required for mouse trophoblast development and mesoderm formation', *Nature*. Nature Publishing Group, 404(6773), pp. 95–99. doi: 10.1038/35003601.

Samarage, C. R. *et al.* (2015) 'Cortical Tension Allocates the First Inner Cells of the Mammalian Embryo', *Developmental Cell*. Cell Press, 34(4), pp. 435–447. doi: 10.1016/J.DEVCEL.2015.07.004.

Sarbassov, D. D. *et al.* (2006) 'Prolonged Rapamycin Treatment Inhibits mTORC2 Assembly and Akt/PKB', *Molecular Cell*. Cell Press, 22(2), pp. 159–168. doi: 10.1016/j.molcel.2006.03.029.

Schöler, H. R. *et al.* (1990) ‘New type of POU domain in germ line-specific protein Oct-4’, *Nature*. Nature Publishing Group, 344(6265), pp. 435–439. doi: 10.1038/344435a0.

Schrode, N. *et al.* (2013) ‘Anatomy of a blastocyst: Cell behaviors driving cell fate choice and morphogenesis in the early mouse embryo’, *genesis*, 51(4), pp. 219–233. doi: 10.1002/dvg.22368.

Schroer, T. A. and Sheetz, M. P. (1991) ‘Two activators of microtubule-based vesicle transport.’, *The Journal of cell biology*. Rockefeller University Press, 115(5), pp. 1309–18. doi: 10.1083/JCB.115.5.1309.

Severance, A. L. and Latham, K. E. (2017) ‘PLK1 regulates spindle association of phosphorylated eukaryotic translation initiation factor 4E binding protein, and spindle function in mouse oocytes’, *American Journal of Physiology - Cell Physiology*, 313(5), p. ajpcell.00075.2017. doi: 10.1152/ajpcell.00075.2017.

Showkat, M., Beigh, M. A. and Andrabi, K. I. (2014) ‘mTOR Signaling in Protein Translation Regulation: Implications in Cancer Genesis and Therapeutic Interventions’, *Molecular Biology International*. Hindawi, 2014, pp. 1–14. doi: 10.1155/2014/686984.

Siller, K. H. and Doe, C. Q. (2008) ‘Lis1/dynactin regulates metaphase spindle orientation in Drosophila neuroblasts’, *Developmental Biology*. Academic Press, 319(1), pp. 1–9. doi: 10.1016/J.YDBIO.2008.03.018.

Skamagki, M. *et al.* (2013) ‘Asymmetric Localization of Cdx2 mRNA during the First Cell-Fate Decision in Early Mouse Development’, *Cell Reports*. Cell Press, 3(2), pp. 442–457. doi: 10.1016/J.CELREP.2013.01.006.

Splinter, D. *et al.* (2012) ‘BICD2, dynactin, and LIS1 cooperate in regulating dynein recruitment to cellular structures’, *Molecular Biology of the Cell*. American Society for Cell Biology, 23(21), pp. 4226–4241. doi: 10.1091/mbc.E12-03-0210.

Starr, D. A. *et al.* (1998) ‘ZW10 helps recruit dynactin and dynein to the kinetochore’, *Journal of Cell Biology*. Rockefeller University Press, 142(3), pp. 763–774. doi: 10.1083/jcb.142.3.763.

Stolovich, M. *et al.* (2002) ‘Transduction of growth or mitogenic signals into translational activation of TOP mRNAs is fully reliant on the phosphatidylinositol 3-kinase-mediated pathway but requires neither S6K1 nor rpS6 phosphorylation.’, *Molecular and cellular biology*. American Society for Microbiology, 22(23), pp. 8101–13. doi: 10.1128/MCB.22.23.8101-8113.2002.

Strumpf, D. (2005) ‘Cdx2 is required for correct cell fate specification and differentiation of trophectoderm in the mouse blastocyst’, *Development*, 132(9), pp. 2093–2102. doi: 10.1242/dev.01801.

Susor, A. *et al.* (2015) ‘Temporal and spatial regulation of translation in the mammalian oocyte via the mTOR-eIF4F pathway’, *Nature Communications*. Nature Publishing Group, 6, pp. 1–12. doi: 10.1038/ncomms7078.

Suwińska, A. *et al.* (2008) ‘Blastomeres of the mouse embryo lose totipotency after the fifth cleavage division: Expression of Cdx2 and Oct4 and developmental potential of inner and outer blastomeres of 16- and 32-cell embryos’, *Developmental Biology*. Academic Press, 322(1), pp. 133–144. doi: 10.1016/J.YDBIO.2008.07.019.

Tarkowski, A. K. (1959) ‘Experiments on the development of isolated blastomeres of mouse eggs’, *Nature*, 184(4695), pp. 1286–1287. doi: 10.1038/1841286a0.

Tarkowski, A. K. (1961) ‘Mouse chimæras developed from fused eggs’, *Nature*, 190(4779), pp. 857–860. doi: 10.1038/190857a0.

Tarkowski, A. K. and Wróblewska, J. (1967) ‘Development of blastomeres of mouse eggs isolated at the 4- and 8-cell stage.’, *Journal of Embryology and Experimental Morphology*, 18(1), pp. 155–180.

Thamodaran, V. and Bruce, A. W. (2016) ‘p38 (Mapk14/11) occupies a regulatory node governing entry into primitive endoderm differentiation during preimplantation mouse embryo development’, *Open Biology*. Royal Society Journals, 6(9), p. 160190. doi: 10.1098/rsob.160190.

Thoreen, C. C. *et al.* (2012) ‘A unifying model for mTORC1-mediated regulation of mRNA translation’, *Nature*. Nature Publishing Group, 485(7396), pp. 109–113. doi: 10.1038/nature11083.

Wang, Q. T. *et al.* (2004) ‘A genome-wide study of gene activity reveals developmental signaling pathways in the preimplantation mouse embryo’, *Dev Cell*. Cell Press, 6(1), pp. 133–144. doi: 10.1016/S1534-5807(03)00404-0.

Watanabe, T. *et al.* (2014) ‘Limited predictive value of blastomere angle of division in trophectoderm and inner cell mass specification’, *Development*, 141(11), pp. 2279–2288. doi: 10.1242/dev.103267.

Waterman-Storer, C. M. *et al.* (1997) ‘The interaction between cytoplasmic dynein and dynactin is required for fast axonal transport.’, *Proceedings of the National Academy of Sciences of the United States of America*, 94(22), pp. 12180–12185. doi: 10.1073/pnas.94.22.12180.

Whited, J. L. (2004) ‘Dynactin is required to maintain nuclear position within postmitotic Drosophila photoreceptor neurons’, *Development*, 131(19), pp. 4677–4686. doi: 10.1242/dev.01366.

Williams, S. E. *et al.* (2011) ‘Asymmetric cell divisions promote Notch-dependent epidermal differentiation’, *Nature*. Nature Publishing Group, 470(7334), pp. 353–358. doi: 10.1038/nature09793.

Yagi, R. *et al.* (2007) ‘Transcription factor TEAD4 specifies the trophectoderm lineage at the beginning of mammalian development.’, *Development (Cambridge, England)*. The Company of Biologists Ltd, 134(21), pp. 3827–36. doi: 10.1242/dev.010223.

Yamamoto, A. *et al.* (1999) ‘A cytoplasmic dynein heavy chain is required for oscillatory nuclear movement of meiotic prophase and efficient meiotic recombination in fission yeast.’, *The Journal of cell biology*. Rockefeller University Press, 145(6), pp. 1233–49. doi: 10.1083/JCB.145.6.1233.

Yamamoto, A. *et al.* (2001) ‘Dynamic Behavior of Microtubules during Dynein-dependent Nuclear Migrations of Meiotic Prophase in Fission Yeast’, *Molecular Biology of the Cell*, 12(12), pp. 3933–3946. doi: 10.1091/mbc.12.12.3933.

Yamanaka, Y. *et al.* (2010) 'FGF signal-dependent segregation of primitive endoderm and epiblast in the mouse blastocyst', *Development*. Oxford University Press for The Company of Biologists Limited, 137(5), pp. 715–724. doi: 10.1242/dev.043471.

Yamashita, R. *et al.* (2008) 'Comprehensive detection of human terminal oligo-pyrimidine (TOP) genes and analysis of their characteristics', *Nucleic Acids Research*, 36(11), pp. 3707–3715. doi: 10.1093/nar/gkn248.

Zernicka-Goetz, M. (2004) 'First cell fate decisions and spatial patterning in the early mouse embryo', *Seminars in Cell & Developmental Biology*. Academic Press, 15(5), pp. 563–572. doi: 10.1016/J.SEMCDB.2004.04.004.

Zernicka-Goetz, M. (2005) 'Cleavage pattern and emerging asymmetry of the mouse embryo', *Nature Reviews Molecular Cell Biology*, 6(12), pp. 919–928. doi: 10.1038/nrm1782.

Zernicka-Goetz, M., Morris, S. A. and Bruce, A. W. (2009) 'Making a firm decision: Multifaceted regulation of cell fate in the early mouse embryo', *Nature Reviews Genetics*. Nature Publishing Group, 10(7), pp. 467–477. doi: 10.1038/nrg2564.